FUEL CYCLE TRANSITION SIMULATION CAPABILITIES IN CYCLUS

BY

JIN WHAN BAE

THESIS

Submitted in partial fulfillment of the requirements
for the degree of Master of Science in Nuclear, Plasma, and Radiological Engineering
in the Graduate College of the
University of Illinois at Urbana-Champaign, 2018

Urbana, Illinois

Master's Committee:

Assistant Professor Kathryn D. Huff, Adviser
Professor James F. Stubbins

Abstract

Recent interest in advanced reactors and the following need for techno-economic transitions has increased the demand for tools necessary to model complex nuclear fuel cycles (NFCs) and advanced reactor technologies. This thesis demonstrates the capability of CYCLUS, the agent-based fuel cycle simulator, to model, simulate, and analyze real-world fuel cycle transition scenarios. This thesis introduces new methods and tools that use various databases to model and simulate real-world nuclear fuel cycle transition scenarios involving advanced reactor technologies.

The work in this thesis contains: (1) benchmarking Cyclus to other nuclear fuel cycle simulators (NFC simulators); (2) developing new methods and tools necessary for modeling and simulating real-world fuel cycle transition scenarios; (3) simulation of both domestic and international nuclear technology transitions.

The methods and tools developed for such capabilities include: (1) modeling and simulating past and current nuclear fleets using historic nuclear reactor operations database; (2) modeling individual reactors and their operating history to calculate nuclear material inventory; (3) modeling Molten Salt Reactor (MSR) behavior in a large-scale fuel cycle simulation.

Benchmark work shows that CYCLUS results coincide with results from other NFC simulators with minor differences due to modeling choices. Additionally, this thesis demonstrates the CYCLUS capability to effectively model and simulate real-world NFC transition scenarios that involve advanced reactor technologies such as MSRs.

Acknowledgments

I consider all my output as a result of me standing on the shoulders of giants. There have been multiple giants that were kind enough to lend me their shoulders. Notably, the tallest of all, my advisor and mentor Kathryn Huff, who patiently guided me from my academic infancy. Also, I owe the world to my parents and loving brother who brought me up with love from my actual infancy. I also thank the staff of Oak Ridge National Laboratory Joushua L. Peterson-Droogh, Eva Davidson, Ben Betzler and Andrew Worrall for their guidance over the summer.

I also cannot express enough gratitude to my friends and colleagues. My greatest assets and partners that I have had the privilege to cohabitate with, Daniel O'Grady and Steven Stemmley, who were the logical anchor in my life. Also, my colleagues Andrei Rykhlevskii, Gwendolyn Chee, Gregory Westphal, Gyu Tae Park, Sun Myung Park, and Anshuman Chuabe have been of great help. Last but not least I thank my long-time friends Jieon Kim, Eric Bae, Daniel Stewart, Corey Burden, Shane Riew, Steve Chung, my comrades from the 12DIV Engineering 3CO, Christine Song, Gyum Hurr and Jae Man Jung.

Table of Contents

List of Tables

List of Figures

Chapter 1

Introduction

The scope of this work includes development and demonstration of various methods and tools to leverage CYCLUS' existing capabilities to model and simulate real-world nuclear fuel cycle transition scenarios involving advanced reactor technologies.

1.1 Background

Increasing climate change concerns have directed attention to nuclear energy, which produces reliable baseload energy with negligible CO_2 emission. To reduce CO_2 emissions, the world will have to reduce fossil fuel power plants. Also, the world energy demand is expected to increase (28% growth between 2015 and 2040 [15]). Given the two circumstances, nuclear power is expected to play a crucial role in the world energy portfolio.

However, concerns of the accumulating UNF inventory, safety of the current reactor fleet, and the availability of uranium resources create a negative public perception of nuclear energy and its sustainability.

Advanced fuel cycles that recycle nuclear fuel provide an opportunity for solving those concerns while meeting energy demand. For the collective goal of transitioning into advanced fuel cycles, the American Nuclear Society (ANS) Fuel Cycle & Waste Management Division (FCWMD) has identified three grand challenges [34], listed below. The grand challenges are identified challenges that members of the society collectively agree need to be resolved by 2030 in order to help solve some of the economic, sociological, or political issues that the nuclear society face [70].

1. Establish used nuclear fuel recycling associated with the "most promising" fuel cycles that are economically competitive with current electricity production.

2. Leverage the findings of the U.S. Department of Energy (DOE)'s Evaluation and Screening Study to reconsider the U.S. approach to the whole nuclear fuel cycle, and publicly establish the "most promising" nuclear fuel cycles and address some of the stretched "truths" about some fuel cycles.

3. Establish a logical incremental timeline toward a pilot and full-scale recycling facility for current reactors, and transition to future reactors from the "most promising" fuel cycles.

The three grand challenges can be summarized as a need to identify and plan for a "most promising" fuel cycle, while accurately calculating its impacts. In 2011, the DOE commissioned a report in order to plan the U.S. nuclear future. The report by Wigeland et al. identified potential fuel cycle groups and compared them to find the most 'promising' fuel cycles [79]. The objective of the evaluation was to provide information about the potential benefits and challenges of nuclear fuel cycle options, in order to guide the DOE Fuel Cycle Research and Development (FCRD) program.

However, this study evaluated fuel cycle statically, such that the material flow and reactor deployment were evaluated at equilibrium. Therefore, the study did not take into account the dynamic changes in fuel demand and reactor deployment or the previously existing fleet. Static fuel cycle analyses fail to capture the utilization of previously existing inventory. Thus, for a more comprehensive and realistic evaluation of a fuel cycle, fuel cycle analyses must include the transition from a previous fleet to the intended fuel cycle. Analysis of fuel cycle transition scenarios can more accurately calculate the dynamic material demands in a transition into a new fuel cycle, thus helps outline fuel cycle Research and Development (R&D) and facility deployment roadmap.

Given this gap, a simulation tool capable of accurately calculating the metrics of a fuel cycle transition scenario is essential for solving these grand challenges. This work will demonstrate capabilities of a system-level analysis tool, CYCLUS. I developed `cyclus-input-gen` to ease CYCLUS input generation of historic nuclear operation. I also developed `saltproc_reactor` to model MSRs in CYCLUS. These added capabilities will streamline modeling of transition scenarios as well as allow CYCLUS to model fuel cycles involving MSRs.

1.1.1 The nuclear fuel cycle

The nuclear fuel cycle is the complete nuclear energy system from mining to disposal [75]. A common goal of a NFC is to produce power economically, while minimizing waste and natural resource used. Other specialized goals of NFCs may involve weapons material production or repository burden reduction through transmutation. The discharge UNF from the reactors is eventually sent back to facilities for either recycling or disposal.

In 2011, the DOE commissioned a report in order to plan the U.S. nuclear future. The report by Wigeland et al. identified potential fuel cycle groups and compared them to find the most 'promising' fuel cycle [79]. The objective of the evaluation was to provide information about the potential benefits and challenges of nuclear fuel cycle options, in order to guide DOE FCRD program. This study identified 40 fuel cycle groups, categorized by the extent of recycling (no recycle, limited recycle, and continuous recycle), fuel composition (e.g. thorium-U233, uranium-plutonium), and the type of reactors (fast/thermal critical reactors, sub-critical Externally Driven Systems (EDS)).

Fuel Cycles can be mainly categorized by their treatment of UNF. A fuel cycle that disposes all UNF generated is

a once-through fuel cycle. If the UNF is reprocessed, a fuel cycle is categorized either as a closed fuel cycle, or a fuel cycle with limited recycling, depending on the number of time the fuel passes through a reactor.

Once-through fuel cycle

In a once-through cycle, nuclear fuel is used once and then sent to storage without further reprocessing [75]. This cycle is often called the open fuel cycle, and is the current cycle for most nations with nuclear energy (e.g. U.S., Korea, Finland, Sweden).

This fuel cycle begins with mining of uranium or thorium ore, which is extracted from the ground. The mined ore is milled to form yellowcake (U_3O_8). The yellowcake is then either converted to UF_6 and enriched, or converted to UO_2 directly. This is because some reactor designs (e.g. Canada Deuterium Uranium (CANDU) designs[73]) can operate with natural uranium, while others (e.g. LWRs) need higher-than-natural levels of uranium-235. The processed UO_2 is then fabricated to pellets and loaded into fuel assemblies.

Once the fuel is depleted in the reactor, it is put in on-site pools to cool down. After cooling, the UNF is stored in dry casks as interim storage, destined to be sent to a geologic repository for permanent disposal.

Closed fuel cycle

In a closed fuel cycle, the UNF is recycled to be reused in a nuclear reactor. Recycling has two major benefits: increased fuel utilization and reduction of repository burden.

A typical composition of UNF discharged from an LWR is approximately 95% uranium, 0.9% plutonium, 0.1% minor actinides, and 4% fission products [22]. The uranium, plutonium, and minor actinides have the capability to produce power through fission. Thus, every group except the fission products can be separated to create new fuel for other reactors.

Additionally, repository capacity is constrained mostly by decay heat load and radioactivity, meaning that removal of the high-activity isotopes leads to a more efficient utilization of the repository capacity. Short-lived fission products (e.g. cesium, strontium) contribute to significant heat and radioactivity in the first 100 years of UNF disposal, and long-lived minor actinides (americium, plutonium), contribute to longer-term heat and radioactivity [80], as shown in figure 1.1.

There are two major reprocessing technologies: methods that use low-temperature chemical separation using organic solvents (e.g. PUREX [5]), and methods that use high-temperature molten salts and metals, like pyroprocessing [46]. These methods separate the UNF into different streams, which are then sent to either a high level waste (HLW) repository (fission products) or an appropriate fuel fabrication facility (plutonium).

Different closed fuel cycles use different elemental groups for recycled fuel fabrication. For example, the PUREX

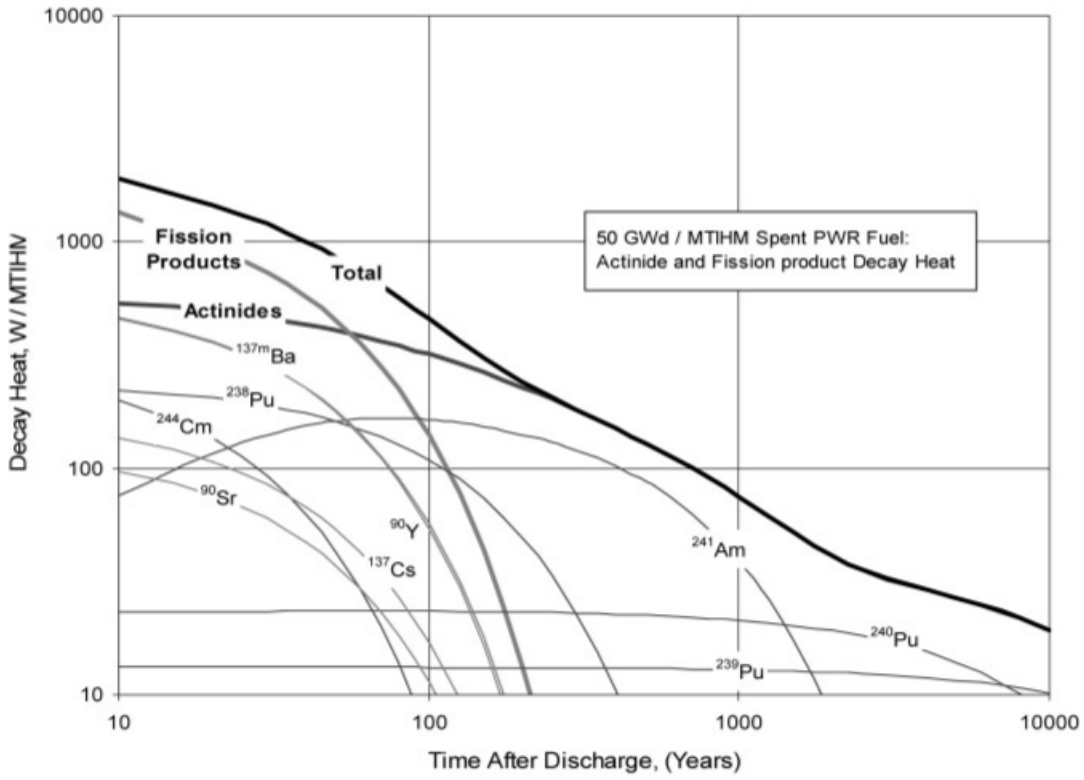

Figure 1.1: Decay heat contributions in UNF from a PWR irradiated to 50 GWd/MTHM. Reproduced from Wigeland, 2006 [80].

process is used in La Hague in France [65], THORP in the U.K [61], Mayak in Russia, and Rokkasho in Japan to separated plutonium and uranium [8]. The plutonium is mixed with either depleted uranium (tails) or reprocessed uranium to produce Mixed Oxide Fuel (MOX).

Closed fuel cycles generally involve fast-spectrum reactors to control TRU inventory. A fast-spectrum reactor can be designed to either burn (reduce TRU), breed (produce more TRU), or break-even (maintain TRU amount). Selection of the fast-spectrum reactor design depends on the goal of the deploying institution.

Fuel cycle with limited recycling

Fuel cycle with limited recycling is defined by the recycling of UNF for a limited number of times. The goals for recycling the irradiated fuel include reusing the separated material in a nuclear reactor and separating long-lived highly radioactive elements for repository burden reduction [79]. The difference between limited recycling and 'closed' fuel cycles (continuous recycling) is the number of cycles fuel might undergo transmutation. In 'closed' fuel cycle, the fuel undergoes many to an infinite number of cycles, through constant reprocessing.

1.1.2 Fuel cycle transition scenarios

In a fuel cycle transition, an initial fleet of technology and corresponding fuel cycle strategies dynamically evolve into a different final state [54]. In this work, I focus on the transition from once-through fuel cycles to closed fuel cycles through the progressive replacement of previous technology (i.e. LWRs) with an advanced technology (i.e. reprocessing and fast-spectrum reactors). Other transition scenarios include a general transition into a different fuel cycle (evaluation group defined by Wigeland et al.), to a mixture of fuel cycles, or a complete nuclear energy phaseout.

In this work, I analyze the material feasibility of fuel cycle transition scenarios, which is characterized by whether all nuclear reactors received fuel on time.

The fuel demand is determined by two factors - nuclear energy demand and the nation's fuel cycle strategy. The nuclear energy demand determines the construction and operation schedule of new reactors, and the fuel demand is calculated accordingly. Fuel cycle strategies determine the isotopic requirements of the fuel cycle transition scenario. For example, if the transition drives toward a U-Pu MOX fuel cycle, plutonium inventory dominates the timescale and feasibility of transition.

Once the expected fuel demand is calculated, the initial condition - current fissile material inventory and number of reactors (and their remaining lifetimes) - determines the material feasibility and timescale of a transition scenario. If a transition scenario is infeasible (i.e. fissile source is lacking) or delayed, the transition can be 'loosened', by delaying deployment of advanced reactors. The energy demand can instead be met by additional deployment of

previous reactor technology (e.g. LWRs), thereby increasing transition timescale but reducing the intensity of fissile material demand.

Since fuel cycles involve multiple facilities, transition scenario analyses require dynamic tracking of materials and facilities. The dynamic tracking will calculate available nuclear material inventory as well as the demand for the nuclear material.

1.1.3 Real-world fuel cycle simulation

Real-world fuel cycle simulation captures the non-uniformity of reactor facilities in the real world. Most work on fuel cycle simulation assumes a uniform fleet of reactors with identical parameters, such as core size and power capacity. This simplification does not reflect the current state of nuclear operation, in which reactors vary in power capacity and core size, leading to errors in UNF inventory and power demand calculations. Capturing the real-world nuclear fleet requires discrete modeling of facilities, with unique parameters for each facility as well as discrete material and facility event (e.g. refuel outage, decommission) modeling.

1.2 Nuclear fuel cycle simulators

NFC simulators are system-level analysis tools that allow tracking of material flow in an NFC. Their functionalities include, but are not limited to, isotopic decay, depletion calculations, and separation of material streams. The goal of a NFC simulator is to calculate *metrics* - quantitative measures of performance that can be compared among fuel cycle options [37].

The obtained metrics can then be optimized to the interests of different stakeholders. Passerini et al. [57] identified categories and criteria for NFC optimization and weighted the criteria for different stakeholders (e.g. Industry, laboratories). This approach can help decide which metric is important to stakeholders and optimize the fuel cycle for that metric.

Table 1.1 lists the NFC simulators considered in this section. The listed NFC simulators generally focus on one functionality (e.g. multi-regional analysis, detailed isotopic tracking, demand-driven deployment, cost analysis, sensitivity study) but lack in the flexibility to perform other functionalities [35]. In other words, no NFC simulator has all the functionalities to perform the superset of analysis types.

1.3 Objectives

This thesis demonstrates and extends the real-world NFC transition scenario modeling capabilities in CYCLUS. The goal of this thesis is to develop tools that leverage CYCLUS' modularity to add capabilities required for modeling

Table 1.1: List of NFC simulators considered in this paper. Reproduced from [35]

Name	Developer	Reference(s)
CAFCA	MIT	[30]
COSI6	CEA (Frane)	[20]
DANESS	ANL	[77]
DESAE2.1	Rosatom (Russia)	[74]
EVOLCODE2	CIEMAT (Spain)	[1]
FAMILY21	JAEA (Japan)	[54]
GENIUSv1	INL	[18]
GENIUSv2	Univ of Wisconsin	[17]
NFCSS	IAEA	[39]
NFCSim	LANL	[64]
VISION	ANL/INL	[43]

real-world fuel cycle transition scenarios. The added capabilities are then demonstrated through NFC transition scenarios relevant to France and the United States.

1.4 Motivation

There are two major motivations for accurately simulating real-world NFC transition scenarios. First, NFC transitions require strategized reactor and fuel cycle deployment to meet fuel demand for advanced systems. A simulation tool must be able to calculate the material and facility throughput requirements of the transition scenario. Second, NFC transition scenarios need to optimize existing investment and technology. For example, with an NFC simulator, analysts can determine the best reactor technology to leverage current LWR UNF inventory in a nation.

1.4.1 Capabilities required for modeling transition scenarios

To meet the two goals mentioned above, a NFC simulator needs to have specific capabilities. A study by Brown et al. [12] identified nine common functionalities of NFC simulators for modeling transition scenarios - material compositions, deployment of fuel cycle facilities, front-end facility models, separations and material recycle facilities, reactor facilities, back-end features, starting the new fuel cycle, materials queuing and prioritization under capacity limitations, and energy demand algorithms. Brown et al. categorize each feature into three tiers - **basic**, **integral**, and **exemplary**. **Basic** features are essential in modeling a fuel cycle, such as conservation of mass in composition changes, facility deployment and retirement, and modeling of front-end facilities like an enrichment facility. **Integral** features are needed to bind the basic functionalities to process transition scenarios. Examples of **integral** features are demand-driven deployment of fuel cycle facilities and material prioritization. Finally, **exemplary** features enable exploration of various sensitivities and technology choices, and are not essential. **Exemplary** features include discrete isotope tracking and radioactive decay.

The functionalities, features, and their hierarchies are organized in table 1.2.

Table 1.2: Nine common functionalities identified for NFC simulator to perform fuel cycle transition scenarios. Reproduced from Brown et al. [12]

Functionality	**Feature**	**Hierarchy**
Composition Features	Explicit modeling of fuel materials including primary fissile and fertile actinide isotopes	Basic
	Fuel's initial heavy metal mass modeled as lumped masses of the remaining actinides and fission products to conserve mass	Basic
	Isotopic decay of materials in storage	Exemplary
	Modeling of intermediate isotopes (e.g. ^{233}Pa)	Exemplary
	Tracking of fission products beyond a simple lumped sum	Exemplary
	Modeling of compounding materials in fuels and waste forms	Exemplary
Fuel Cycle Facility Deployment	Facility deployment and retirement	Basic
	Construction time delays	Basic
	Strategic deployment to meet demand	Integral
Front-end Facilities	Source (mining and milling)	Basic
	Details of mines and mills including annual and total quantities available	Exemplary
	Conversion and enrichment facilities	Basic
	Timing and capacity of recycle facilities	Basic
	Fuel fabrication	Basic
	Time delays and losses in separations and fabrication	Basic
Separations and Material Recycling	Separations facilities may be required for UNF	Basic
	Cooling time	Basic
	Losses in separations	Basic
	Material selection from the UNF supply	Basic

Table 1.2 (cont.)

Reactor Facility	Fueling: number of batches, cycle length and fuel per batch	Basic
	Multiple fuel types in reactor facility (driver, blanket)	Basic
	Pre-generated charge and discharge isotopic compositions	Basic
	Real time calculations based on reactor physics models	Exemplary
	Reactor facility lifetime, construction time, and decommissioning time	Basic
	Initial charge for first core and discharge for final core	Basic
Back-end	Cooling of used fuel	Basic
	Conservation of mass - consistency with charged mass and generated power	Basic
Fuel Cycle Startup	External source of fissile material	Basic
	Startup on recycled fuel from other facilities	Integral
	Primary and back-up fuel types	Exemplary
Material Prioritization	Material accumulation	Basic
	Material prioritization	Integral
	Radioactive decay	Exemplary
Energy Demand Algorithm	Technology allocation accounting for availability	Integral
	Ordering and deployment of multiple reactor technologies	Integral

1.4.2 Additional capabilities identified for real-world fuel cycle transition scenarios

I have identified three additional functionalities beyond those identified by Brown et al. [12] for modeling real-world NFC transition scenario - integrating historical data, modeling discrete facilities and events, and modeling liquid-fueled reactors with continuous reprocessing.

Integrating historical data

In modeling real-world nuclear fuel cycle transition scenarios, initial conditions (e.g. existing fissile inventory, existing reactor fleet) strongly impact the transition scenario parameters, such as reactor deployment schemes, fuel types, and reactor designs. This requires the NFC simulator to correctly model the current fleet and its remaining lifetime. The purpose of a fuel cycle is to produce power, thus the objective function of a fuel cycle simulation is generally to meet a certain power demand. Once the required installed capacity of the current fleet is calculated, the analyst can determine the deployment scheme of future reactors to meet a future power demand.

Past work on modeling real-world fleets

Modeling real-world fleets requires data about the current existing fleet, such as power capacity, first criticality date, core size, and expected shutdown date.

A study by Sunny et al. modeled the current U.S. nuclear fleet using ORION [71]. However, the fleet represented by Sunny et al. is far from modeling real-world U.S. nuclear fleet since it assumed a deployed LWR capacity of 90 GWe in 2015, which decreases by 5 GWe every year starting from 2030, meaning that no consideration is given to the actual shutdown dates of existing reactors. This simplification stems from ORION modeling reactors as a fleet governed by a power demand, not as discrete facilities.

Another U.S. NFC transition scenario simulation by Worrall [82] models actual U.S. nuclear fleets using the Power Reactor Information System (PRIS) database, which is the same method used for this work. However, the analysis is done using an extensive network of spreadsheets, and not a NFC simulator.

Modeling real-world fleets is possible in CYCLUS, for two reasons. First, CYCLUS models discrete facilities with their own events and material flow. Second, CYCLUS has a text-based input file structure, meaning that the input files (and thus the scenario) can be generated from a database and a script, as in this work.

Discrete reactor facility modeling

Discrete modeling of reactors allows a higher resolution of the power supply and material flow. In the real world, especially in the United States, existing reactors do not have the same power output or core size. This means that lumping the reactor fleet together causes a loss in accuracy. The loss in accuracy occurs by not capturing phenomena such as anisotropic fresh fuel fabrication requirements, spent fuel isotopics of a fleet of reactors with greatly varying burnups, and chaotic isotopic balance in fuel cycles involving multiple recycling passes [35]. COSI 6 [20], EVOLCODE [1], FAMILY21 [54], have discrete facility modeling capabilities, while DESAE2.2[74], and VISION [43] do not [10].

Similarly, most NFC simulators do not treat disruption events (lack of fuel supply or decommissioning of a reactor) discretely. For example, ORION shuts down the entire simulation if there is a lack of fuel supply, and cannot decommission reactors mid-cycle. DESAE 'borrows' lacking fuel from storage (leaving a negative mass value) instead of shutting down the reactor [50]. COSI models reactors operating in sync [9].

Modeling liquid-fueled reactors with continuous reprocessing

MSR designs have recently gained attention due to their potential to be safer, more efficient in heat conversion, and sustainable [67]. Multiple companies in the U.S. are now pursuing commercialization of MSR design reactors, such as Terrapower, Terrestrial [47], and Thorcon [44]. Other parties such as China (TMSR-LF [16]) , France (REBUS-3700

[53]), and the European Union (MSFR [32], MOSART [42]) are developing MSR designs.

However, modeling an MSR is challenging due to its on-line reprocessing and continuously flowing fuel. The material flow in and out of the reactor is continuous and dynamic, as well as the composition inside the core. Neutronics and depletion calculations have to be performed continuously while the composition of the fuel changes via depletion and reprocessing. Reactor physics and depletion calculations on MSRs have been done. For example, Oak Ridge National Laboratory researchers developed ChemTriton [60], a python script that drives SCALE, to perform semi-continuous reprocessing of the fuel [59, 7]. However, modeling MSRs in an NFC simulator is a challenge due to the significant computational burden associated with frequent depletion calculations.

This challenge of large computational time in an NFC simulator can be overcome by 'outsourcing' the computationally heavy work to the higher-fidelity reactor physics and depletion codes. In such a workflow, the high-fidelity code simulates a certain MSR design for its lifetime, while recording the history of its feed and waste in a database. A CYCLUS facility module reads this database and mimics the feed and removal behavior listed in the database, effectively modeling MSR material flow. This allows MSR modeling in a larger-scale system analysis without heavy computational burden, while securing fidelity of the depletion calculation.

1.5 Methods

This thesis accomplishes the objective in three steps. First, a benchmark showed good agreement with other fuel cycle simulation tools. [1] Second, I identified and developed the tools and methods necessary for modeling and simulating real-world transition scenarios. Finally, I constructed and ran fuel cycle transition scenarios relevant to France and the United States to demonstrate and verify the capability.

1.5.1 Benchmark study

A previous study by Feng et al. [23] validates existing NFC simulators in a fuel cycle transition scenario, in which an LWR fleet transitions into an SFR fleet with continuous reprocessing. This study compares four well-known NFC simulators DYMOND [83], VISION [43], ORION [28], and MARKAL [68]. The results from each code were compared to a set of 'model solutions' that were generated from a spreadsheet for various metrics (e.g. fuel loading in reactor, UNF inventory). I reproduced the transition scenario in CYCLUS, and compare the CYCLUS results with those from the model solutions.

[1] These results have been submitted for publication in Annals of Nuclear Energy.

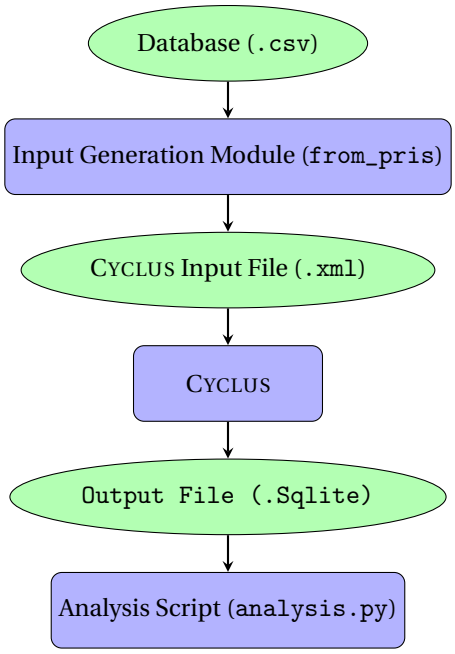

Figure 1.2: Green circles and blue boxes represent files and software processes, respectively, in the computational workflow.

1.5.2 Tool development

In order to model real-world transition into an advanced fuel cycle, two major tools were developed. First, I developed a python package `cyclus-input-gen`, which includes the submodule `from_pris` that automates extraction from the curated International Atomic Energy Agency (IAEA) PRIS database [40]. Second, I developed `saltproc_Reactor`that models MSRs in CYCLUS using a database generated from a high-fidelity MSR depletion calculation.

1.5.3 Real-world fuel cycle transition scenario simulation

Fuel cycle transition scenarios for France and the United States were constructed. I made different assumptions for the two scenarios to account for each nation's different goals, initial conditions (i.e. currently existing fleet, UNF inventory), and their potential reactor technology. The python package `from_pris` was used to construct the initial CYCLUS input file, followed by iterations to account for new reactor deployment. The workflow driving the analyses is shown in diagram 1.2.

The structure of this thesis is as follows. In chapter 2, I review other fuel cycle simulation tools and their gaps, and explain the unique capability CYCLUS has for transition scenario simulation. Chapter 3 discusses the design and development of capabilities needed for NFC transition simulation. Chapter 4 describes the results from the benchmark study, in which CYCLUS results are compared to results from other fuel cycle simulation tools. Chapter 5

and 6 details the results from the France and United States fuel cycle transition scenarios, in which each nation's LWR fleet transitions into a fast reactor fleet with continuous reprocessing.

Chapter 2

Tools used for this work

2.1 CYCLUS

CYCLUS is an agent-based nuclear fuel cycle simulation framework [37], meaning that each reactor and fuel cycle facility is modeled as a discrete and independent player in the simulation. A CYCLUS agent archetype defines the logic that governs the behavior of an agent. In this simulation, the user defines the archetype's parameters. The archetypes with user-defined parameters are then deployed as agent prototypes. Encapsulating the `Facility` agents are the `Institution` and `Region`. A `Region` agent holds a set of `Institutions`. An `Institution` agent can deploy or decommission `Facility` agents.

Several versions of `Institution` and `Region` agents exist, varying in complexity and purpose [36]. `DeployInst`, which deploys agents at user-defined timesteps, serves as the main `Institution` archetype in this work. All reactor `Facility` agents, fuel reprocessing, and fabrication `Facility` agents are deployed through `DeployInst`, while basic fuel cycle `Facility` agents such as sink, source, enrichment, and storage facilities are deployed through `NullInst`, which simply deploys `Facility` agents at the beginning of the simulation.

At each timestep, agents make requests for materials or bid to supply them and exchange with one another. A market-like mechanism called the dynamic resource exchange [27] governs the exchanges. For output analysis, each material resource has a quantity, composition, name, and a unique identifier.

In this work, each nation is represented as a `Region` agent, that contains `Institution` agents, which deploy `Facility` agents according to a user-defined deployment scheme.

Cyclus has multiple advantages over other available NFC simulators codes including open-source distribution, modularity, and extensibility. Its agent-based modeling approach is ideal for modeling coupled, physics-dependent supply chain problems common in NFCs. The framework allows for dynamic loading of external libraries, which allows the users to plug-and-play different types of physics models for NFC simulation.

2.1.1 Open source distribution

License agreements and institutional approval are needed for most NFC simulators like COSI, DANESS, DESAE, EVOLCODE, FAMILY21, NFCSim, ORION and VISION [43], challenging both use and development in an academic setting. On the other hand, CYCLUS relies completely on open source, free libraries, allowing all users to both use and develop the Cylcus framework and existing libraries. The open-source distribution of CYCLUS encourages collaboration - any user can propose improvements or contribute extensions for CYCLUS.

2.1.2 Modularity and extensibility

In most modern NFC simulators, the facilities and their behaviors (and their fidelities) are confined in the software. Also, most modern NFC simulators model fuel cycles (once-through, continuous reprocessing) with immutable connections between facilities. On the other hand, CYCLUS allows users to plug-and-play various agent models within the CYCLUS framework (shown in figure 2.1). Also, CYCLUS relies on a market-based model for material trades between facilities, so the user can design any novel fuel cycle. This enables CYCLUS to simulate any system analysis involving multiple connected facilities with physics-based calculations.

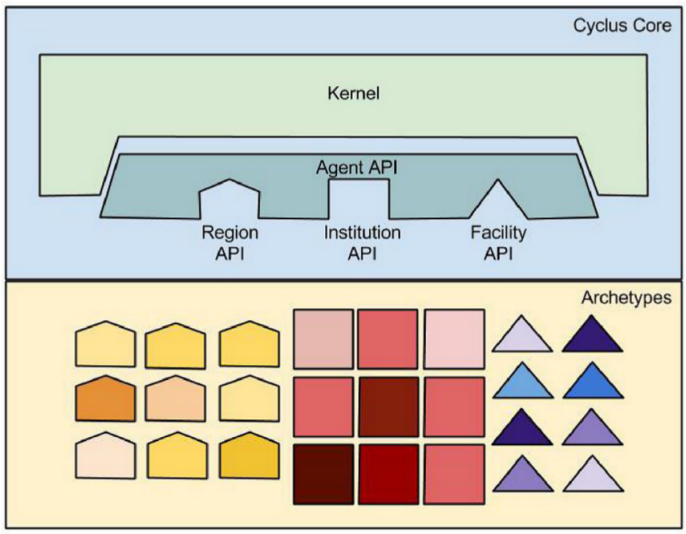

Figure 2.1: The CYCLUS core provides APIs that the archetypes can be loaded into the simulation modularly [37].

Within the CYCLUS kernel, the dynamic resource exchange (DRE) connects the framework and the agents by mediating agent material offers and requests. The kernel solves the multicommodity exchange problem posed by the material offers and requests and executes the transaction between two agents.

2.1.3 Cyclus' fitness for real-world NFC transition scenarios

The CYCLUS framework and its extension libraries fulfill all the functionalities specified by Brown et al. [12]. Additionally, CYCLUS capability to read text-based input structure and model facilities discretely allow modeling of real-world, individual reactors. Modularity in CYCLUS enables adding an MSR model without altering CYCLUS itself.

2.2 SaltProc

SaltProc is an on-line reprocessing simulation driver for SERPENT2 [48] developed by Andrei Rykhlevskii, for simulating liquid-fueled MSR operation [62]. SaltProc uses a semi-continuous approach to simulate continuous MSR material feed and removal [63]. It is coded in Python (compatible with both Python 2 and 3), and records feed, removal, and in-core isotopic history in an HDF5 [29] database.

SaltProc's structure and capabilities are similar to that of the ChemTriton tool for SCALE, developed at ORNL [6]. The computationally heavy work - Monte Carlo neutron transport and burnup calculations - is done in SERPENT, while SaltProc parses through the output material compositions, processes the fuel (removal and feed), and creates a new SERPENT input file. The user can specify removal rates, feed rates, and removal efficiencies for each isotope. At each timestep, the following stream composition vectors are recorded in the database:

- depleted core
- depleted core after reprocessing
- removal stream (reprocessed elements)
- feed stream

The logical flow of SaltProc is illustrated in figure 2.2. Initially, SaltProc reads a user-defined SERPENT 2 input file that contains parameters such as geometry, non-fuel component composition, neutron population, criticality cycles, depletion time, total power, and boundary conditions. SERPENT 2 then performs neutron transport and depletion calculations and returns the number density of the depleted fuel. SaltProc then reads the depleted composition, writes the composition in the database, processes the depleted material according to a user-defined scheme, and then outputs a new fuel composition input card for SERPENT 2. This again is then read by SERPENT 2 and the cycle continues until the user-defined timestep is reached.

One of the benefits of having a semi-continuous external driver for SERPENT 2 is that the user can set up SaltProc so that the density of a certain isotope in the fuel remains constant. In other words, the feed rate can vary over time to meet a certain 'quality' of the fuel. Also, using a Monte Carlo code such as SEPRENT allows users to vary geometric fidelity, from a single cell model to a full core model.

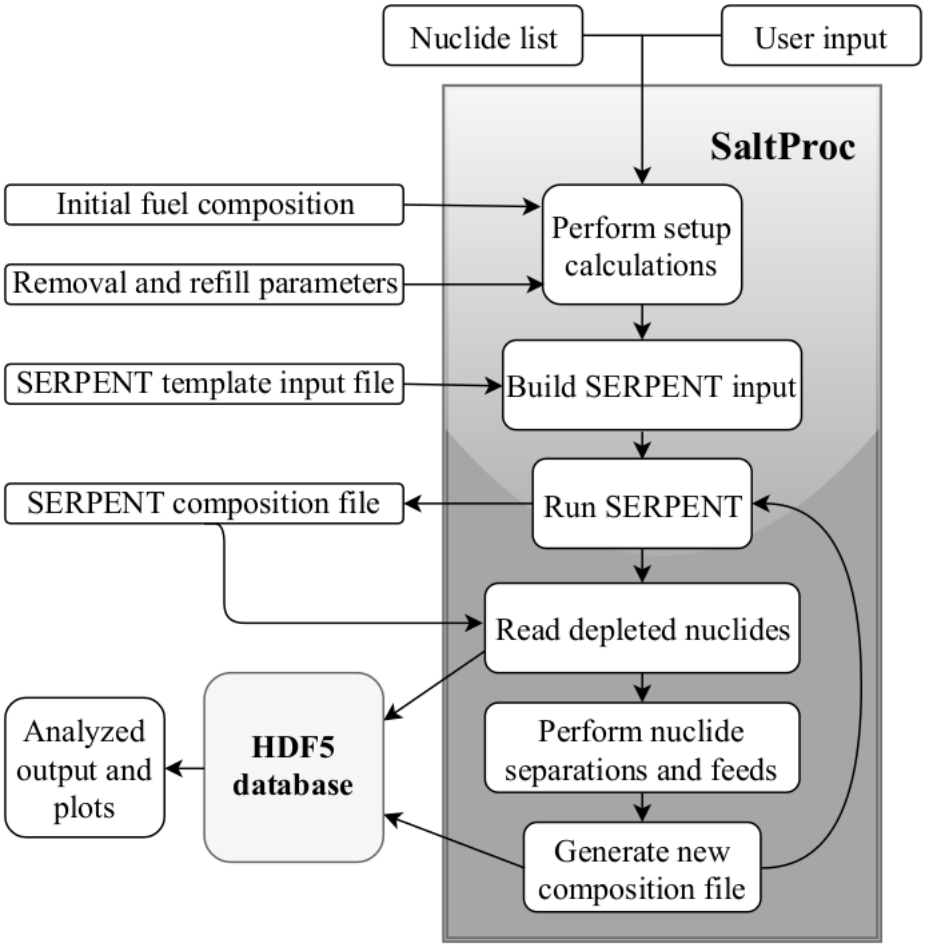

Figure 2.2: Flow chart for the SaltProc tool [63].

2.2.1 Use in this work

SaltProc's output (in HDF5 [29] format) can be imported through a CYCLUS module to mimic the MSR feed and removal behavior throughout its lifetime. The composition in the core is not important here since the data of interest in a system-level NFC simulation is the material flow in and out of the reactor. This method can effectively model MSRs in a large system-scale NFC simulation without significant computational burden for the NFC simulation at run-time.

Chapter 3

Tools developed for this work

I developed two extensions to leverage the capabilities of CYCLUS to model real-world fuel cycle transition scenarios. The first extension is a python input-generating module that automates scenario generation of the real-world nuclear fleet at any point in time. The second extension is a CYCLUS archetype that mimics MSR feed and removal behavior using an HDF5 database generated from SaltProc.

3.1 `cyclus-input-gen`

The python package `cyclus-input-gen` contains multiple submodules for automating CYCLUS input generation. The submodule `from_pris` automates the generation of CYCLUS input files to model the state of reactor fleets at a given point in time.

The script reads from the Power Reactor Information System (PRIS) database [40] and extracts data about each reactor's country, reactor unit, type, net capacity (MWe), status, operator, construction date, first criticality date, first grid date, commercial date, and shutdown date (if applicable). The user inputs simulation configurations such as start year, start month, and simulation duration. `from_pris` uses the collected data to fill out a template into a CYCLUS input file. Diagram 3.1 shows the logical flow of the module.

3.1.1 Reactor deployment calculation

The module calculates the deployment scheme of reactors and their lifetimes by assuming that all reactors shut down after 60 years of operation. If the expected shutdown date is later than the user-input simulation start date, the reactor is not written in the input. If the reactor was operational prior to the simulation start date, and its shutdown date later than simulation start date, the reactor is deployed at the beginning of simulation with its remaining lifetime. If the reactor's start date is later than the simulation start date, and the shutdown time is undefined, the reactor is deployed at the defined start date with 60 years of lifetime.

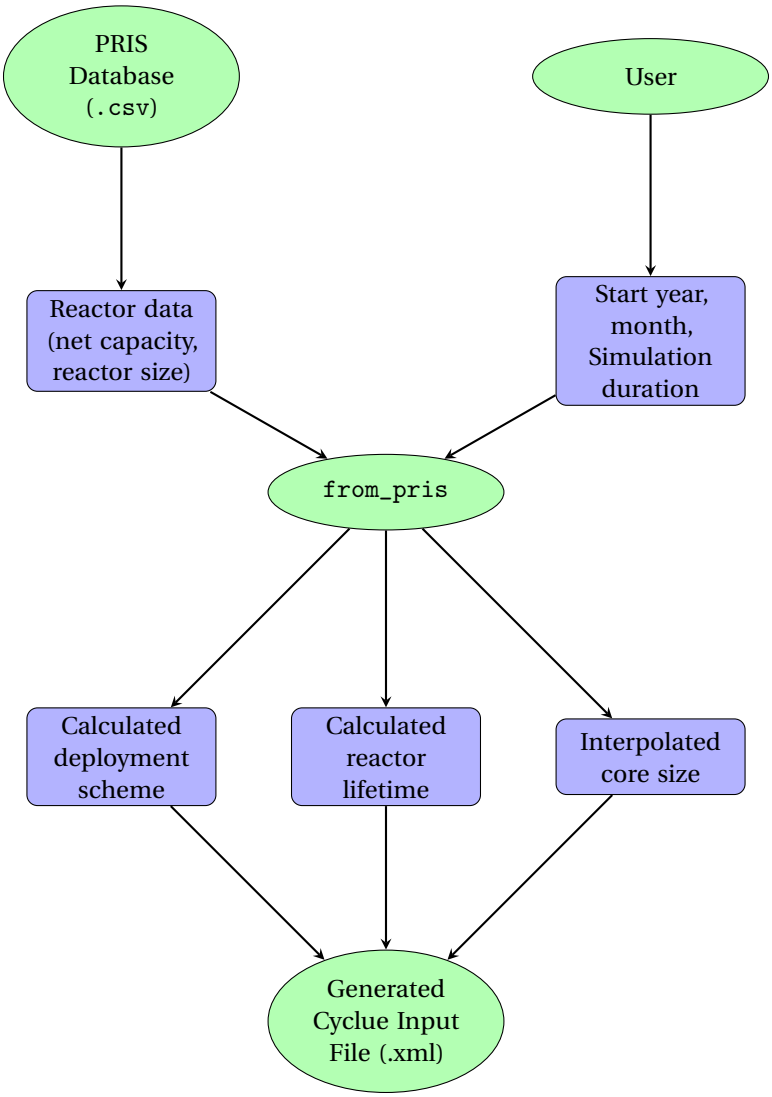

Figure 3.1: Logic flow of `from_pris`. Green circles and blue boxes represent files and data, respectively.

3.1.2 Reactor parameter calculation

The module calculates the core sizes of various reactor types by using a linear core size model. It assumes that the number of assemblies in a reactor core scales linearly from a model reactor design, as shown in the equation below. The mass per assembly is kept constant. The model reactor designs are listed in table 3.1.

$$A = A_{ref} \cdot \frac{\mathrm{P}}{P_{ref}}$$

$$N_{assem.pwr} = 157 \cdot \frac{\mathrm{P}}{1,100}$$

$$N_{assem.bwr} = 764 \cdot \frac{\mathrm{P}}{10,098}$$

$$N_{assem.phwr} = 4,560 \cdot \frac{\mathrm{P}}{700}$$

A = number of assemblies in approximated core

P = power capacity of reactor

Table 3.1: Reactor model designs used for the linear core size model.

Category	**Model Reactor**	**Power [MWe]** (P_{ref})	**Assembly Mass [kg]**	**Assemblies in Core** (A)	**Reference**
PWR	AP-1000	1,110	446	157	[66]
BWR	4-MK I	1,098	180	764	[52]
PHWR	CANDU6	700	24.17	4,560	[25]

3.2 saltproc_reactor

The SaltProc reactor is a CYCLUS facility archetype designed to model MSR behavior using a database. It roughly couples "SaltProc" [63] and CYCLUS, by using the output from SaltProc to mimic MSR feed and removal behavior in CYCLUS.

This method is similar to the simplified implementation of recipe reactors, in which the depletion calculation is performed outside of the fuel cycle simulation. Instead of a single depletion calculation used in a recipe reactor, this reactor uses a database of recipes to capture the continuously varying state of liquid-fueled reactors like MSRs.

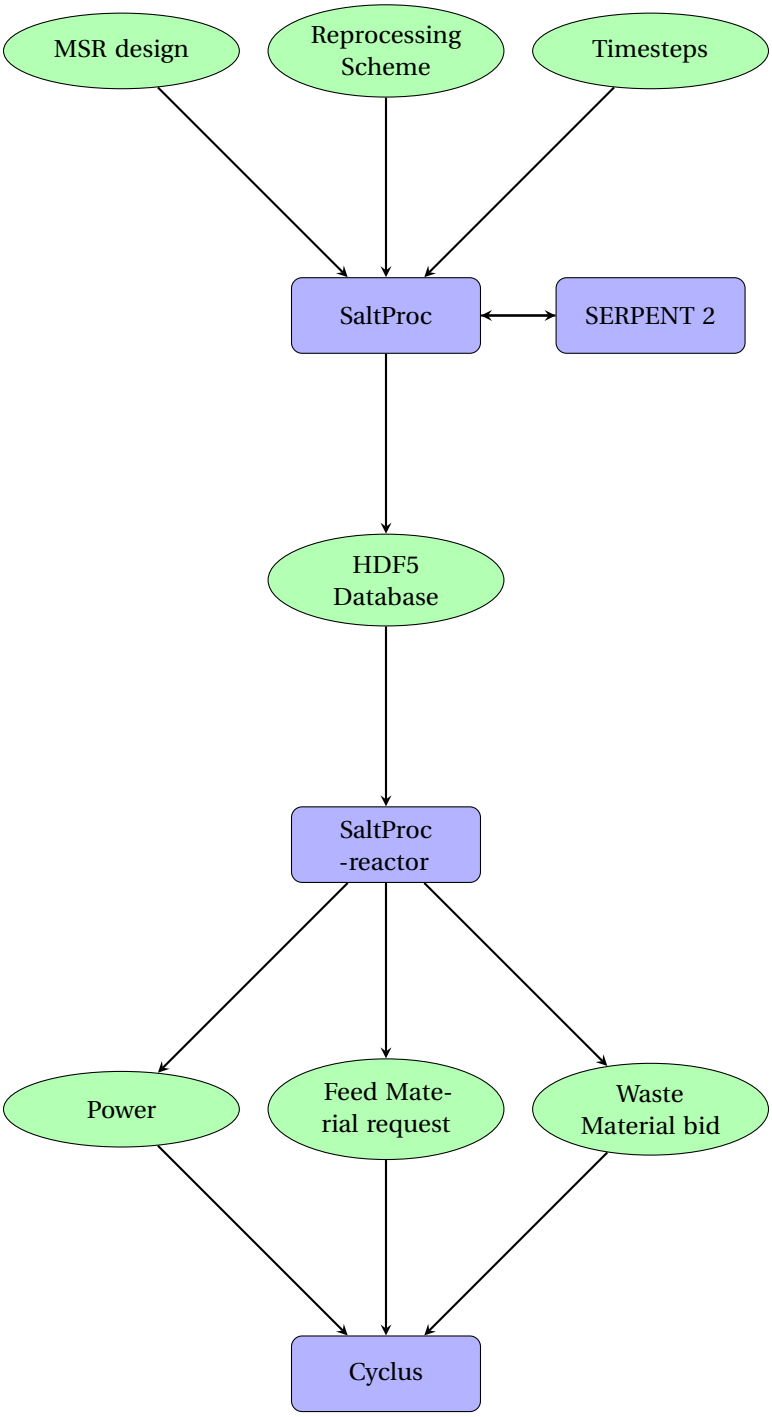

Figure 3.2: Logic flow of `SaltProc Reactor`. Green circles and blue boxes represent files and data, respectively.

3.2.1 Code description

The user provides only of the commodity names for each stream (e.g. waste, fertile), and the database path, since the HDF5 database already contains the notion of reactor design, reprocessing scheme, and other reactor parameters (shown in figure 3.2). The commodity names are needed for reactor agents to communicate with other CYCLUS agents in exchanging material.

At every timestep, The `SaltProc Reactor` calculates the material mass and composition accumulated during the CYCLUS timestep, as shown in equation below.

$$M_T = \sum m_T$$

$$m_T = \sum_{t=(T-1)}^{T} m_t$$

M_T = total mass of stream in one CYCLUS timestep

m_T = mass of isotope in one CYCLUS timestep

m_t = mass of isotope in one SaltProc timestep

3.3 Limitation of the database approach

The limitation of this database approach is that it does not take into account the changing incoming fuel compositions due to decay. The separated TRU composition may vary depending on the duration an LWR UNF assembly has been cooled, thus affecting the performance of the MSR. The database approach assumes a fixed input salt composition, which is not the case in this simulation, because reprocessed TRU has varying decay times from discharge when it is fabricated and put in the MSR.

This limitation is similar to that of recipe reactors, in which the fuel is transmuted to a pre-generated recipe regardless of the incoming fuel composition. For example, a recipe reactor depleting a MOX fuel would deplete the MOX fuel to the same composition regardless of its fresh fuel composition.

There are three alternative to the database approach that can improve the accuracy of MSR depletion modeling:

1. Use collection of databases to cover varying incoming fuel composition
2. Perform depletion calculations in CYCLUS via coupling with SaltProc
3. Perform depletion calculations in CYCLUS using ROMs of depletion codes

The first method can take into account the varying incoming fuel compositions by implementing multiple SaltProc outputs instead of one. In this method, upon receiving initial fuel, CYCLUS would identify the SaltProc output with the initial fuel composition closest to that of the received fuel, which will be more accurate than having only one database that represents one initial composition. However, this method will be difficult to be effective due to the large range of variations that the MSR initial fuel composition can have.

The second method to couple CYCLUS with SaltProc can improve the inaccuracy from varying input fuel compositions, since the exact composition of the fuel received by the reactor facility is depleted in SaltProc, rather than assuming an initial composition. However, since fuel cycle analyses model multiple facilities simultaneously, the computational burden required to run multiple SaltProc simulations simultaneously inside a CYCLUS simulation will outweigh its benefits. Because fuel cycle analyses aim to obtain a 'good-enough' approximation of a large system, coupling CYCLUS with a high-fidelity model and largely increasing the computational burden and simulation time is not preferred.

A compromise of the two previously mentioned methods is implementing a ROM of a high-fidelity depletion model in CYCLUS. A ROM is a statistically trained algorithm that defines a feature space (input parameters) and a target space (output values). The benefit of a ROM is the reduction in computational burden. A ROM can be trained by training from a set of SERPENT depletion results, where the feature space is the input of the simulation, and output is the depleted fuel composition (shown in figure 3.3. The difficulty of creating a ROM for depletion calculations is that the feature space and the target space is very large, since the feature and target space comprise of the composition of every isotope.

In conclusion, each method for modeling MSR depletion in a large scale fuel cycle simulation has unique benefits and drawbacks. The currently implemented method of using a database generated from a high-fidelity depletion tool has its limitations, but is adequate for a fuel cycle simulation, due to its low computational burden and medium fidelity.

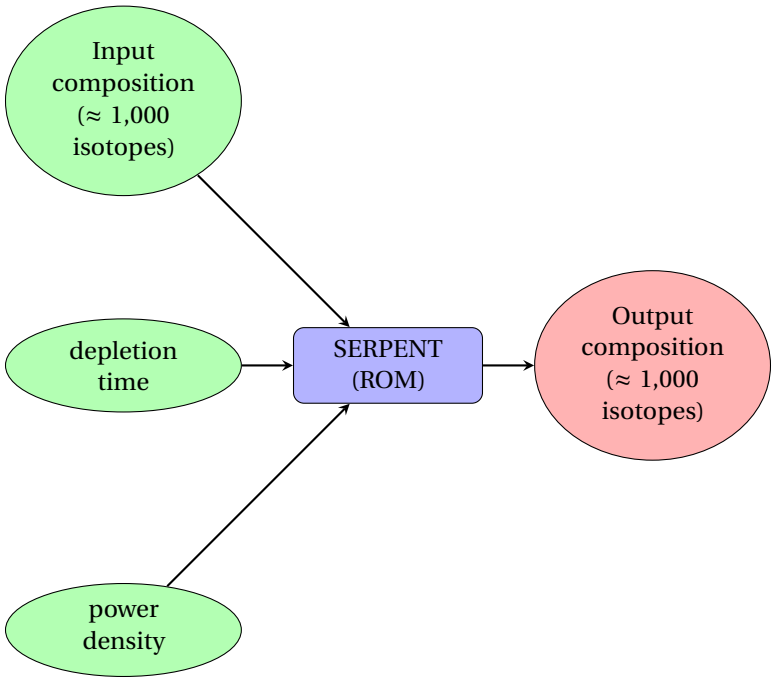

Figure 3.3: Example of a ROM generated from SERPENT results. The green objects represent the feature space, and the red objects represent the target space. This example assumes that the geometry (and any other parameter) is the same for all SERPENT simulations.

Chapter 4

Cyclus benchmark study

I performed a benchmark study comparing CYCLUS' results to results from other NFC simulators to verify CYCLUS and identify modeling differences.

This chapter demonstrates CYCLUS' agreement with other NFC simulators by benchmarking the results of CYCLUS to a previous verification study by Feng et al. [23]. This verification study compared four well-known NFC simulators DYMOND [83], VISION [43], ORION [28], and MARKAL [68]. The results from each code were compared to a set of 'model solutions' that were generated from a spreadsheet for various metrics (e.g. fuel loading in reactor, UNF inventory) in a transition scenario. I took the input parameters from this study, reproduced the transition scenario in CYCLUS, and compared the results. Results show that Cylcus' results are in good agreement with the results from Feng et al., with minor differences caused by reactor module behavior, which is independent of the framework.

4.1 Methodology

Feng et al. comprehensively defined simulation parameters sufficient to reproduce the transition scenario in CYCLUS. In this study, I used the CYCAMORE [37] archetype library to model all fuel cycle facilities. CYCAMORE libraries are archetypes maintained by the core developer team.

In this study, I analyzed the CYCLUS results using python. The post-processed output data was overlain with the results with the model solution from the verification study [23], which was obtained through personal contact with benchmark author Bo Feng at Argonne National Laboratory. The input file and analysis procedures are all available on Github [4].

4.2 Fundamental modeling differences in CYCLUS

CYCLUS has fundamental modeling differences from the fuel cycle analysis codes used in the benchmark [23].

CYCLUS has a default time step of one month. The verification study solutions are evaluated with 1-year time steps, so cumulative and annual averages were used.

The CYCAMORE recipe reactor depletes half of its core when decommissioned mid-cycle, whereas the codes in the benchmark [23] deplete all their reactors' fuel when decommissioned. For this study, I changed the CYCAMORE `Reactor` source code to deplete all its assemblies to the depleted recipe. Also, the CYCAMORE recipe reactor treats each batch (and assembly) as a discrete material, while some codes have continuous fuel discharge. This produces differences in the results because the batches in the benchmark [23] are in time-averaged values. In this study, the LWR batch size and cycle time are increased, while decreasing the batch number to keep the core size constant. I rounded up the SFR batch number, while the batch size and cycle time are kept constant. This increases the core size by 1.08%, which is negligible, but will be discussed in the results section. The differences are listed in table 4.1.

Table 4.1: Difference in Batch number and core size

Category	**Benchmark[23]**	**CYCLUS**
LWR Batches	4.50	3.00
LWR Batch size [tHM]	19.91	29.86
LWR Core size [tHM]	89.59	89.59
LWR Cycle time [years]	1.00	1.50
SFR Batches	3.96	4.00
SFR Batch size [tHM]	3.95	3.95
SFR Core size [tHM]	15.63	15.80

Note that the CYCLUS framework code never needed to be changed. The only change made was the CYCAMORE reactor depletion behavior at decommission. The goal of this study is to show current CYCLUS agreement with other codes and identify differences, not to alter CYCLUS to match the other codes.

4.3 Results

Figure 4.1 shows the deployed reactor capacity, and figure 4.2 shows the LWR retirement and SFR deployment. The two plots show exact agreement with the benchmark solutions.

Figure 4.3 shows the annual fuel loading rate. The initial fuel loading for 100 LWR reactors are not shown in the plot for either the benchmark or the CYCLUS results. The oscillations caused by the 18 month refueling period were aggregated into 12 month groups. As a result the total fuel loaded is equal for both plots.

Although indistinguishable in figure 4.3, there is a 1.08% difference between SFR fuel loading proportional to the core mass difference, because CYCLUS only has integer batch numbers. Figure 4.4 shows the differences normalized by the core mass differences, overlapped with the SFR deployment. This shows that the differences only occur during deployment due to the difference in core mass.

Figure 4.5 shows the inventory of discharged UNF in the mandatory cooling stage (four years for LWR, one year for SFR). It also oscillates around the benchmark's solution and converges, due to the influx and the outflux of UNF

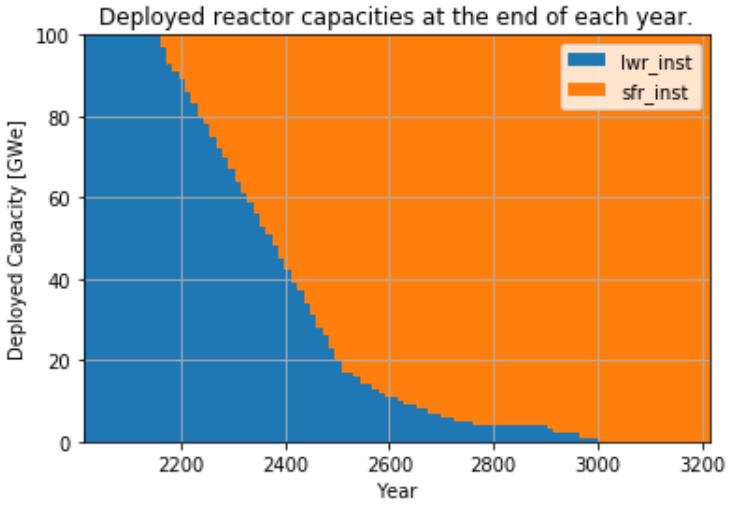

Figure 4.1: Deployed reactor capacities at the end of each year from CYCLUS.

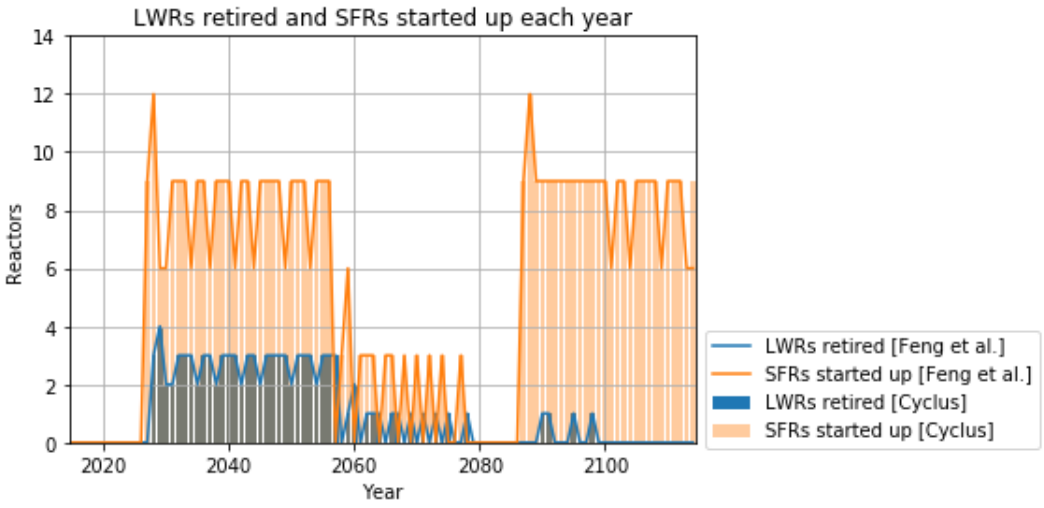

Figure 4.2: LWRs retired and SFRs started up each year.

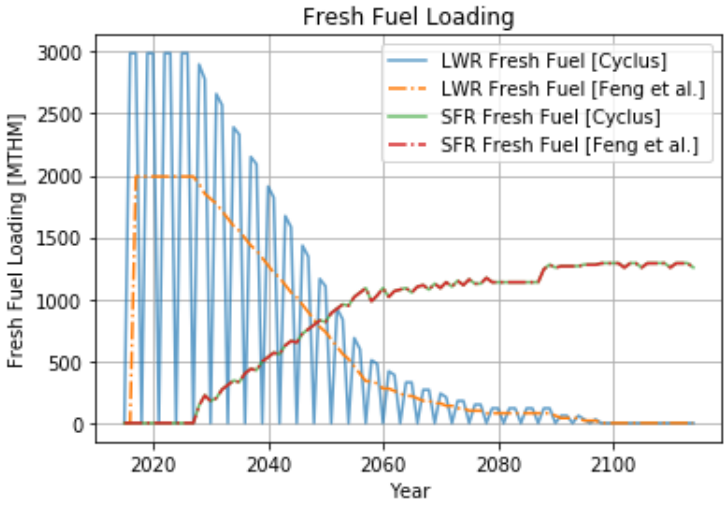

Figure 4.3: Annual fresh fuel loading rates (first cores and reload fuel).

into and out of the storage facility. The SFR inventory and fuel loading solutions exactly matches the benchmark solutions, minus the small (1.08%) difference due to core size.

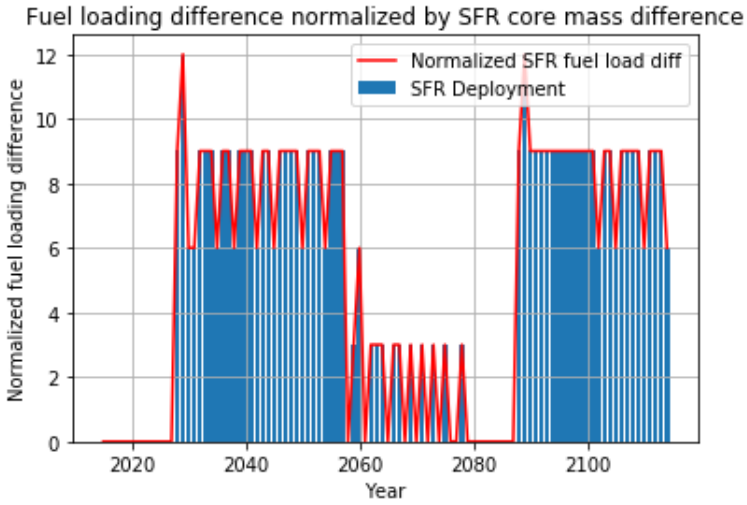

Figure 4.4: Difference between annual fresh SFR fuel loading rates (Cyclus - Benchmark) normalized by the core mass difference of an SFR due to fractional batch size.

Figure 4.6 shows the amount of cooled UNF waiting for reprocessing. The value is calculated by subtracting the cumulative difference between the cooled inventory and the UNF reprocessing throughput.

$$M_w(t) = M_c(t) - M_r(t)$$

$M_w(t)$ = Mass of UNF waiting for reprocessing at time t.

$M_c(t)$ = Mass of UNF under mandatory cooling at time t.

$M_r(t)$ = Mass of UNF reprocessed at time t.

The oscillation is between the cooled inventory in the storage facility before (high) and after (low) the storage facility sends its inventory for reprocessing.

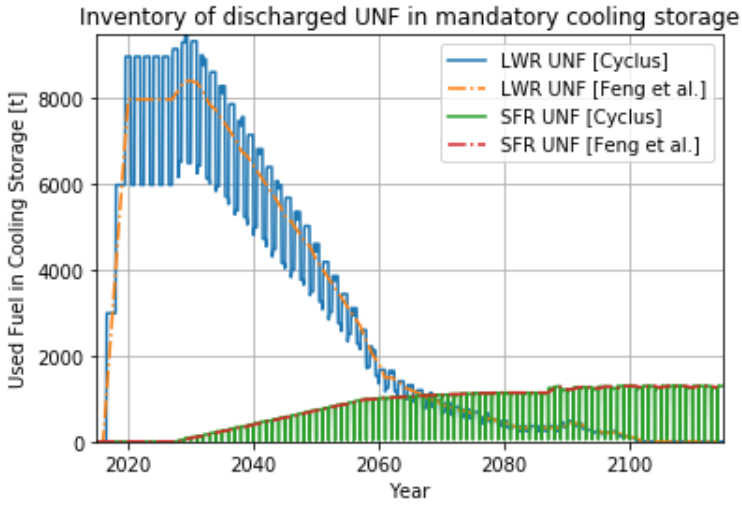

Figure 4.5: Inventory of discharged UNF in mandatory cooling storage.

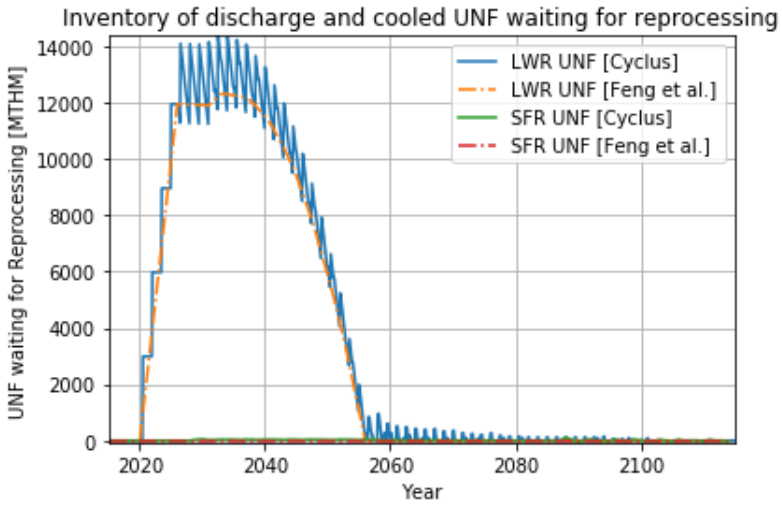

Figure 4.6: Inventory of discharged and cooled UNF waiting for reprocessing.

Figure 4.7 shows the reprocessing throughput, which oscillates around the benchmark solution. No oscillation

exists from 2030 to 2055 because the LWR UNF reprocessing plant throughput peaks at 2,000 tons per year, meaning that the reprocessing plant is at always at full capacity for those times.

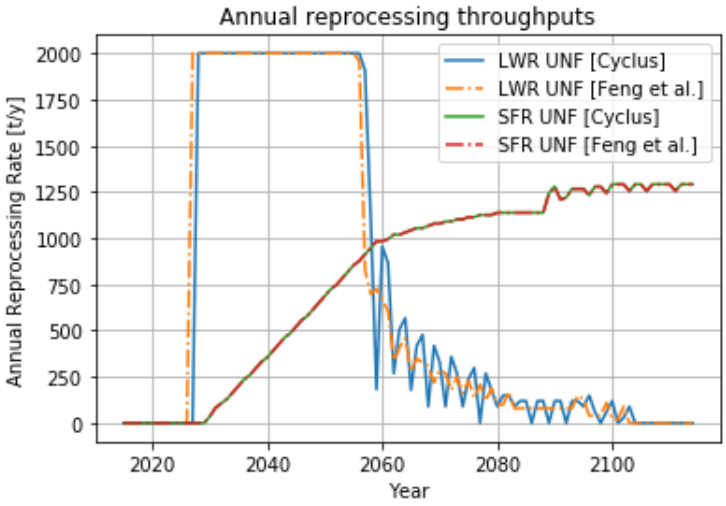

Figure 4.7: Annual reprocessing throughputs.

Figure 4.8 shows the inventory of unused TRU recovered from UNF. The CYCLUS results follow the benchmark solutions closely. However, the larger SFR core size in CYCLUS causes CYCLUS results to be 1.08% smaller than the benchmark results, since more TRU is used to start up the newly deployed SFRs. Note that since batch numbers are integer by their nature, it is unrealistic to have a non-integer batch number. Therefore, the integer restriction in CYCLUS more accurately represents reality.

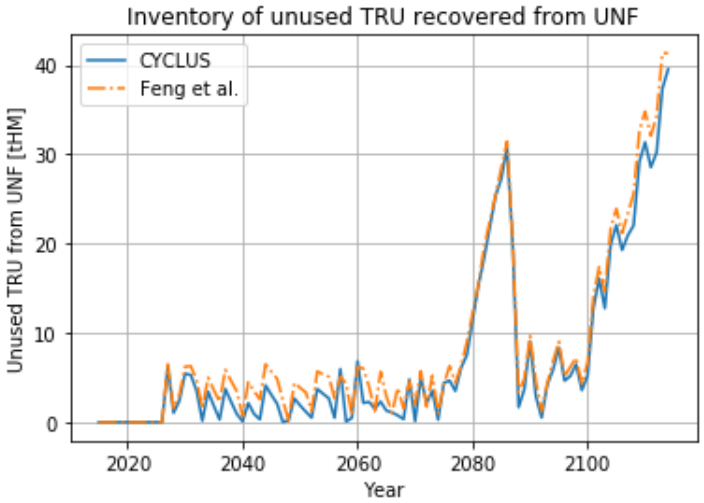

Figure 4.8: Inventory of unused TRU recovered from UNF.

4.4 Discussion

I verified CYCLUS with results from an established verification study and saw good agreement in a transition scenario.

Throughout this work, two major differences were identified that led to the deviation of CYCLUS results from that of the benchmark solution. First, the CYCAMORE reactor depletes only half of its core when decommissioned. Second, CYCLUS, unlike other codes examined in the benchmark (except ORION), fully resolves discrete batches for fuel discharge. I resolved the first discrepancy by changing one line in the Cycamore module source code.

This study proves that CYCLUS is a capable tool for modeling fuel cycle transition scenarios.

Chapter 5

French NFC transition scenario with EU regional analysis

The stated long term plan for nuclear deployment in France targets a technology transition to SFRs[14]. However, the current inventory of French UNF is insufficient to fuel that transition without building new LWRs.

If instead, France accepted UNF from other EU nations and used it to produce MOX for new SFRs, the MOX created will fuel a French transition to an SFR fleet and allow France to avoid building additional LWRs.

I used CYCLUS to simulate EU spent nuclear material inventory accumulation and to model the proposed French technology transition from LWRs to SFRs. I calculated the used fuel inventory in EU member states and propose a potential collaborative strategy of used fuel management.

Past research focuses solely on France and typically assumes that additional LWRs, namely European Pressurized Reactors (EPRs), supply the UNF required to produce MOX [13, 49, 24, 51]. The strategies in these works estimate full SFR transition in 2100. Other recent work in the literature investigates partitioning and transmutation in a European context, with Accelerator-Driven Systemss (ADSs) and Gen-IV reactors [21, 2], to reduce radiotoxicity for disposal. However, little recent work considers synergistic international spent fuel arrangements. This work finds that a collaborative strategy can reduce the need to construct additional LWRs in France, if the SFRs are as commercially competitive as recent work suggests they may be [84].

This chapter details that French NFC transition scenario from an LWR fleet to a fully SFR fleet. I show that if France accepts UNF from other EU nations, it will reach its desired SFR end-goal more rapidly.

5.1 EU deployment schedule

The historic EU deployment schedule and operation history are generated using the `from_pris.py` module (described in section 3.1).

Projections of future reactor deployment in this simulation are based on assessment of analyses from references, for instance PRIS, for reactors planned for construction [41], the World Nuclear Association [3], and literature concerning the future of nuclear power in a global [45] and European context [31]. Existing projections extend to 2050.

Table 5.1 lists the reactors that are currently planned or under construction in the EU. In the simulation, all planned constructions are completed without delay or failure and reach a lifetime of 60 years.

Table 5.1: Power reactors under construction and planned. Replicated from [3].

Exp. Operational	Country	Reactor	Type	Gross MWe
2018	Slovakia	Mochovce 3	PWR	440
2018	Slovakia	Mochovce 4	PWR	440
2018	France	Flamanville 3	PWR	1600
2018	Finland	Olkilouto 3	PWR	1720
2019	Romania	Cernavoda 3	PHWR	720
2020	Romania	Cernavoda 4	PHWR	720
2024	Finland	Hanhikivi	VVER1200	1200
2024	Hungary	Paks 5	VVER1200	1200
2025	Hungary	Paks 6	VVER1200	1200
2025	Bulgaria	Kozloduy 7	[1]AP1000	950
2026	UK	Hinkley Point C1	EPR	1670
2027	UK	Hinkley Point C2	EPR	1670
2029	Poland	Choczewo	N/A	3000
2035	Poland	N/A	N/A	3000
2035	Czech Rep	Dukovany 5	N/A	1200
2035	Czech Rep	Temelin 3	AP1000	1200
2040	Czech Rep	Temelin 4	AP1000	1200

For each EU nation, I categorized the growth trajectory from “Aggressive Growth” to “Aggressive Shutdown”. “Aggressive growth” is characterized by a rigorous expansion of nuclear power, while “Aggressive Shutdown” is characterized as a transition to rapidly de-nuclearize the nation’s electric grid. I categorized each nation’s growth trajectory into five degrees depending on G, the growth trajectory metric:

$$G = \left\{ \begin{array}{ll} \text{Aggressive Growth,} & \text{for } G \geq 2 \\ \text{Modest Growth,} & \text{for } 1.2 \leq G < 2 \\ \text{Maintenance,} & \text{for } 0.8 \leq G < 1.2 \\ \text{Modest Reduction,} & \text{for } 0.5 \leq G < 0.8 \\ \text{Aggressive Reduction,} & \text{for } G \leq 0.5 \end{array} \right\} = \frac{C_{2040}}{C_{2017}}$$

G = Growth Trajectory [−]

C_i = Nuclear Capacity in Year i [$MegawattElectric(MWe)$].

The growth trajectory and specific plan of each nation in the EU is listed in Table 5.2.

[1] The fate of many planned reactors is uncertain. The proposed reactor types are also unclear. The ones marked ‘N/A’ for type are assumed to the PWRs in the simulation.

Table 5.2: Projected nuclear power strategies of EU nations [3]

Nation	Growth Trajectory	Specific Plan
UK	Aggressive Growth	13 units (17,900 MWe) by 2030.
Poland	Aggressive Growth	Additional 6,000 MWe by 2035.
Hungary	Aggressive Growth	Additional 2,400 MWe by 2025.
Finland	Modest Growth	Additional 2,920 MWe by 2024.
Slovakia	Modest Growth	Additional 942 MWe by 2025.
Bulgaria	Modest Growth	Additional 1,000 MWe by 2035.
Romania	Modest Growth	Additional 1,440 MWe by 2020.
Czech Rep.	Modest Growth	Additional 2,400 MWe by 2035.
France	Modest Reduction	No expansion or early shutdown.
Slovenia	Modest Reduction	No expansion or early shutdown.
Netherlands	Modest Reduction	No expansion or early shutdown.
Lithuania	Modest Reduction	No expansion or early shutdown.
Spain	Modest Reduction	No expansion or early shutdown.
Italy	Modest Reduction	No expansion or early shutdown.
Belgium	Aggressive Reduction	All shut down 2025.
Sweden	Aggressive Reduction	All shut down 2050.
Germany	Aggressive Reduction	All shut down by 2022.

Using this categorization to drive facility deployment, CYCLUS captures regional differences in reactor power capacity and UNF production as a function of time. Accordingly, figure 5.1 shows the resulting simulated installed capacity in EU nations. Sudden capacity reductions seen in the 2040s result from end-of-license reactor retirements and nuclear phaseout plans in nations such as Germany and Belgium.

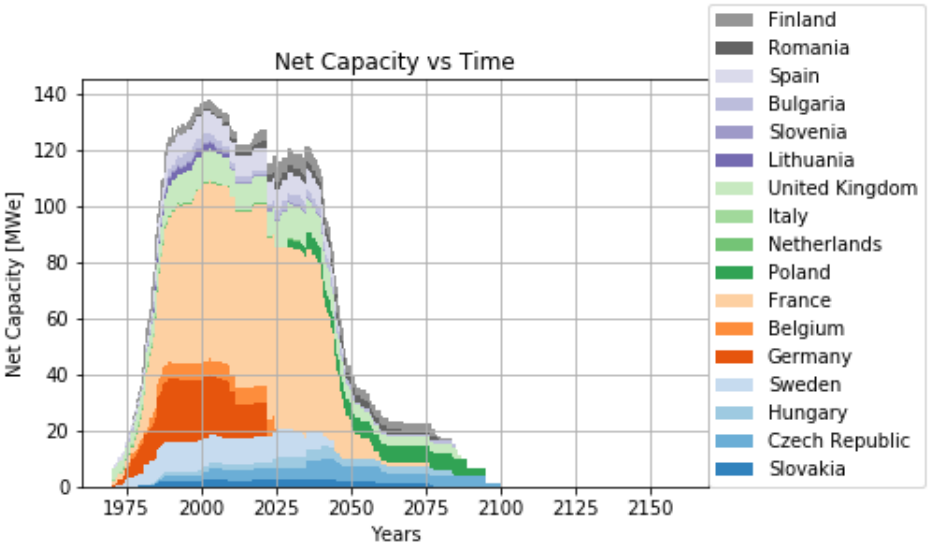

Figure 5.1: Installed nuclear capacity in the EU is distinguished by `Regions` in CYCLUS. The large drops near 2025 is due to the nuclear phase-out plans in Germany and Belgium.

5.2 French SFR deployment schedule

Figure 5.2 shows the French transition to SFRs modeled in this simulation. Historically aggressive growth of nuclear in the 1980s leads to a substantial shutdown of nuclear in the 2040s, which, in the simulation, are replaced by new SFRs. The net capacity is kept constant at 64.7 GWe.

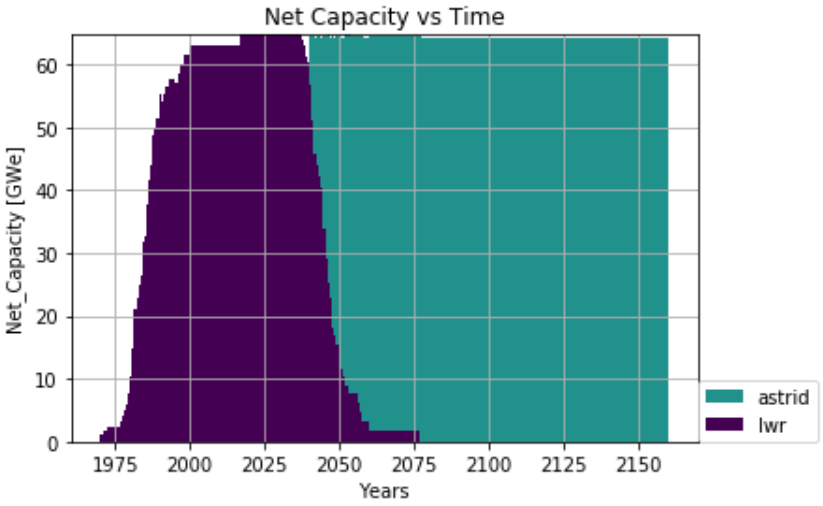

Figure 5.2: The potential French transition from LWRs to SFRs when assisted by UNF from other EU nations.

Figure 5.3 shows the deployment strategy required to support the transition in figure 5.2. France must build 1.78 ASTRIDs per year, on average, to make up for the end-of-license decommissioning of power plants built in the 1980s and 1990s. The second period of aggressive building occurs when the first generation of SFRs decommission after 80 years. Starting in 2040, France deploys 600-MWe SFRs to make up for decommissioned French LWR capacity. This results in an installed SFR capacity of 64,700 MWe by 2078 when the final LWR is decommissioned.

Finally, figure 5.4 shows the total deployment scheme I simulated. The French transition to SFRs couples with the historical and projected operation of EU reactors. The steep transition from 2040 to 2060 reflects the scheduled decommissioning of reactors built in the 1975-2000 era of aggressive nuclear growth in France.

These figures reflect that, for the given assumptions, bursts of construction are necessary to maintain capacity. In reality, a construction rate of five reactors every year is ambitious, but might have the advantage of larger scale production of components and more modular assembly and construction if major components can mostly be built off site.

Alternatively, the deployment of new SFRs can be spread out by staggering scheduled decommissioning of LWRs through lifetime extensions. For example, I increased the original lifetime of French LWRs (60 years) randomly by sampling from a uniform distribution of lifetime extension magnitudes between 0 and 25 years. This results in a

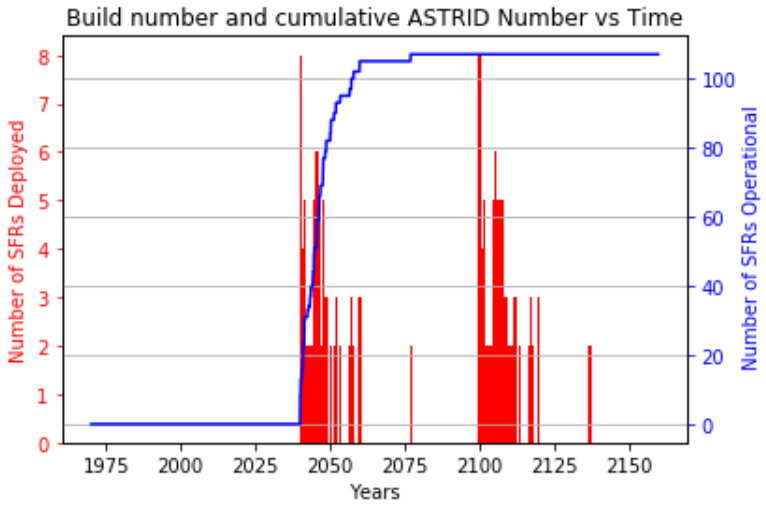

Figure 5.3: The simulated deployment of SFRs in France is characterized by a period of aggressive building.

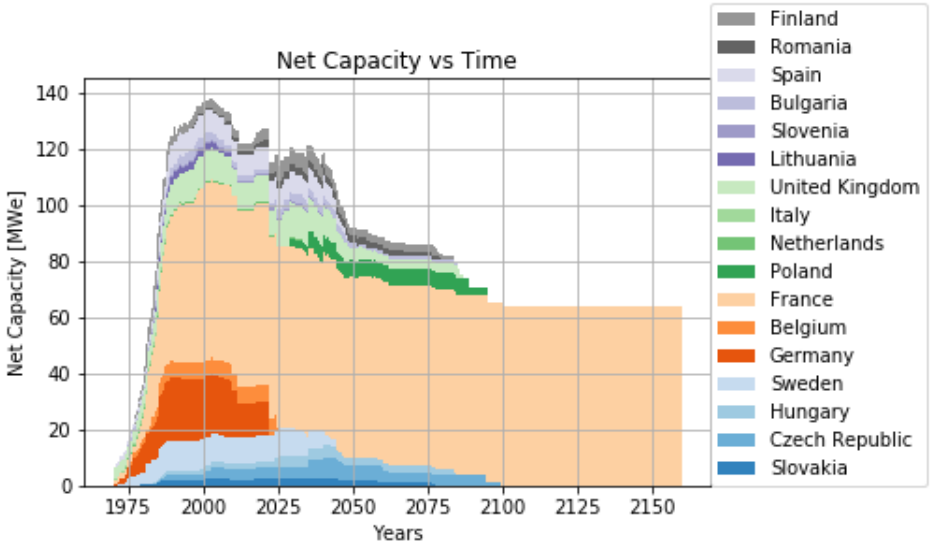

Figure 5.4: The total simulated deployment scheme relies on UNF collaboration among nations.

more gradual transition and ASTRID construction burden, as shown in figure 5.5 and 5.6. The effect of LWR lifetime extension is discussed in Section 5.8.2.

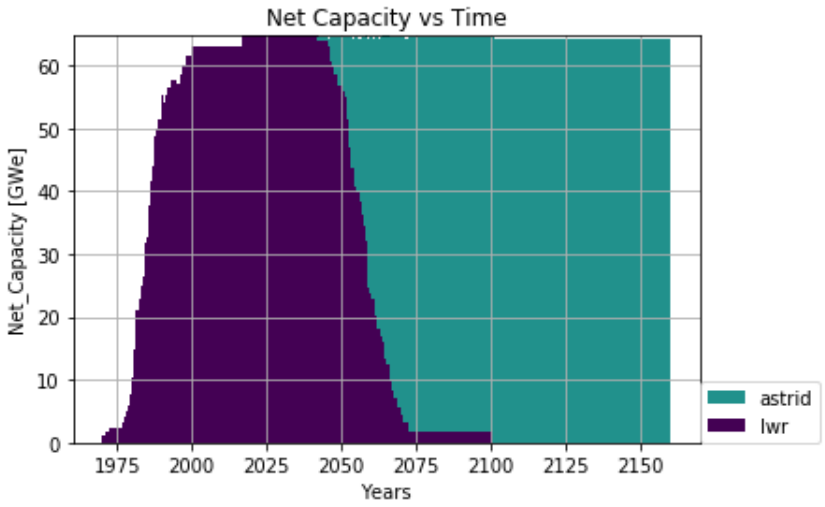

Figure 5.5: The transition to ASTRIDs becomes more gradual if the French LWR lifetime extensions are sampled from a uniform distribution $\in [0,25]$ years.

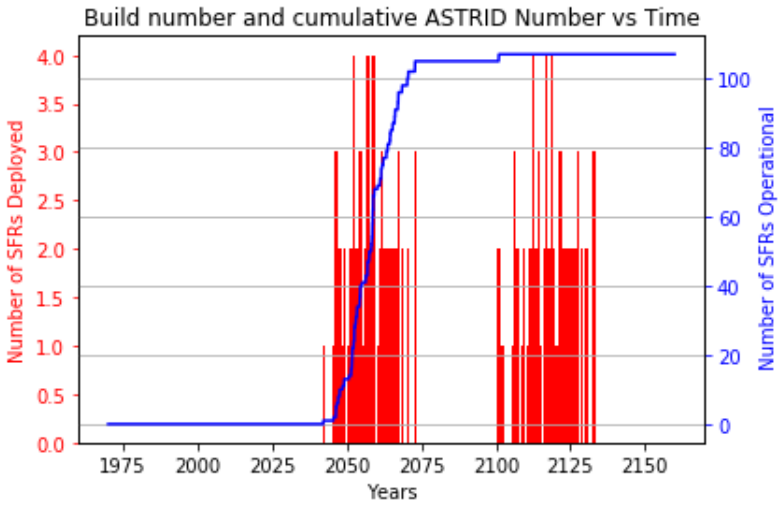

Figure 5.6: The acute construction burden lessens if the French LWRs lifetime extensions are sampled from a uniform distribution $\in [0,25]$ years.

This analysis establishes a multi-national material flow and demonstrates that, if such an aggressive deployment scheme took place, the SFRs would have enough fuel.

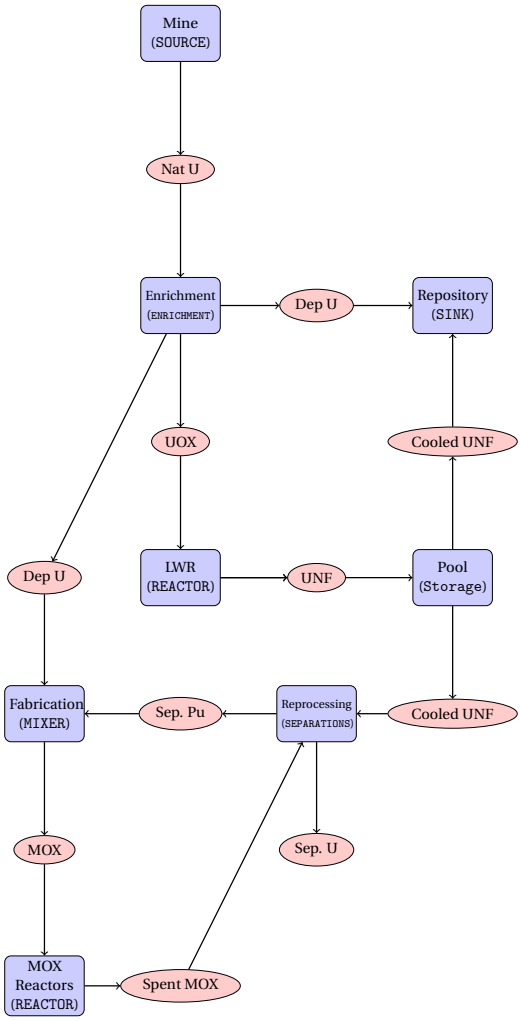

Figure 5.7: Fuel cycle facilities (blue boxes) represented by CYCLUS archetypes (in parentheses) pass materials (red ovals) around the simulation.

5.3 Material flow

The fuel cycle is represented by a series of facility agents whose material flows are illustrated in figure 5.7, along with the CYCLUS archetypes that were used to model each facility. In this diagram, MOX Reactors include both French PWRs and SFRs.

A mine facility provides natural uranium, which is enriched by an enrichment facility to produce UOX. Enrichment wastes (tails) are disposed of to a sink facility representing ultimate disposal. The enriched UOX fuels the LWRs which in turn produce spent UOX. The used fuel is sent to a wet storage facility for a minimum of 72 months. [13].

The cooled fuel is then reprocessed to separate plutonium and uranium, or sent to the repository. The plutonium mixed with depleted uranium (tails) makes MOX (Both for French LWRs and ASTRIDs). Reprocessed uranium

is unused and stockpiled. Uranium is reprocessed in order to separate the raffinate (minor actinides and fission products) from usable material. Though neglected in this work, reprocessed uranium may substitute depleted uranium for MOX production. In the simulations, sufficient depleted uranium existed that the complication of preparing reprocessed uranium for incorporation into reactor fuel was not included. However, further in the future when the depleted uranium inventory drains, reprocessed uranium (or, natural uranium) will need to be utilized.

5.4 Scenario specification

The scenario specifications defining the simulations presented in this work are listed in table 5.3. The reprocessing and MOX fabrication capacity in France prior to 2020 is modeled after the French La Hague and MELOX sites [65, 38].

Table 5.3: Simulation Specifications

Specification	**Value**	**Units**
Simulation Starts	1970	year
Simulation Ends	2160	year
Production of ASTRID fuel begins	2020	year
SFRs become available	2040	year
Reprocessed uranium usage	Not used	-
Minimum LWR UNF cooling time	72	months
Minimum ASTRID UNF cooling time	36	months
Separation efficiency of U and Pu	99.8	%
Reprocessing streams	Pu and U	-
Reprocessing capacity before 2020	91.6 [65]	MTHM/month
Reprocessing capacity after 2020	183.2	MTHM/month
LWR MOX fabrication throughput	16.25 [38]	MTHM/month
ASTRID MOX fabrication throughput	No limit (∞)	MTHM/month
LWR MOX recycling	Not reprocessed	-
ASTRID MOX recycling	∞-pass	-

5.5 Reactor specifications

Three major reactors are used in the simulation, PWR, BWR, and ASTRID-type SFR reactors. The PWR and BWR specifications are determined using the linear core size model, as explained in section 3.1. The ASTRID-type SFR specification is obtained from Varaine et al [78]. The ASTRID design's target lifetime is 60 years [26].

Table 5.4: Baseline LWR and ASTRID simulation specifications.

Specification	**PWR [72]**	**BWR [33]**	**SFR** [78]
Lifetime [2] [y]	60	60	60
Cycle Time [mos.]	18	18	12
Refueling Outage [mos.]	2	2	2
Rated Power [MWe]	1110	1000	600
Assembly mass [kg]	446	180	–
Batch mass [kg]	–	–	5,568
Discharge Burnup [GWd/tHM]	51	51	105
Assemblies per core [3]	157	764	–
Batches per core	3	3	4
Initial Fissile Loading [t]	4.3 ^{235}U	5.8 ^{235}U	4.9 Pu
Fuel	UOX or MOX	UOX	MOX

5.6 Material definitions

Depletion of the nuclear fuel is modeled with pre-calculated spent fuel recipes, such that a fresh and used fuel recipe are defined for each reactor type. An ORIGEN reference calculation provides the composition of the used fuel (see table 5.5). ORIGEN calculates buildup, decay, and processing of radioactive materials [56]. This recipe has also been used for repository performance modeling [81].

Table 5.5: Fresh fuel compositions in the simulation [81, 78].

	Composition [%]		
Recipe	U235	U238	Pu
Fresh UOX Fuel	4.29	95.71	0.0
Fresh LWR MOX Fuel	0.2	90.7	9.1
Fresh ASTRID Fuel	0.3	77.7	22.0

5.7 Results

This section describes the simulation results if France utilized UNF from other EU nations to fuel the transition into a fully ASTRID fleet.

[2] The simulated reactor lifetime reaches the licensed lifetime unless the reactor is shut down prematurely.

[3] Number of assemblies and corresponding LWR core masses are reported for a 1100-MWe core. Reactors with different core powers are modeled with a linear mass assumption.

First, I confirm that France does not have enough LWR UNF to transition into a fully SFR fleet. As shown in figure 5.8, France cannot meet the ASTRID fuel demand without receiving LWR UNF from other EU nations. France is able to fuel some of its ASTRIDs and breed more plutonium, but cannot meet the fuel demand of all ASTRIDs with this aggressive deployment scheme.

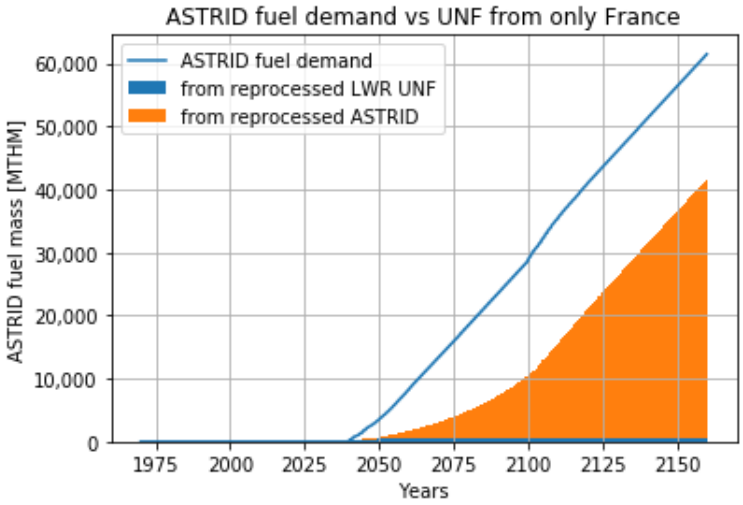

Figure 5.8: ASTRID fuel demand compared with fuel supply from only France in the simulation. The lack of initial ASTRID fuel is caused by the lack of LWR UNF to reprocess. The initial shortage then causes a decrease in plutonium bred by ASTRIDs, thus a decrease in ASTRID fuel supply.

Nuclear fuel material inventory

Table 5.6 lists predicted EU material inventory in 2050. While UNF continues to accumulate after 2050, the UNF France receives before 2050 is most impactful for the feasibility of the transition. Note that table 5.6 distinguishes the stored UNF from the UNF reprocessed to create MOX.

Table 5.6: EU nuclear material inventory in 2050.

Category	**Value [MTHM]**	Specifics
UOX Loaded	152,271	UOX used in EU reactors 1970-2050
MOX Loaded	6,463	MOX used in French reactors 1970-2050
Available used UOX (EU)	85,111	Used EU (minus France) UOX in storage for future ASTRID MOX production
Available used UOX (France)	12,582	Used French UOX stored for future ASTRID MOX production.
Reprocessed UOX (France)	51,511	Used French UOX already reprocessed for the production of LWR MOX
Tails	1,330,165	(Tails generated) − (Tails used for production of LWR MOX)
Natural U Used	1,482,436	

Figures 5.9 and 5.11 show the accumulation of tails and used fuel over time in the EU. Tails accumulate as a by-product of uranium enrichment. Spent fuel is discharged from reactors every refueling period. The entire core is discharged when the reactor decommissions. A total of 1,330,165 MTHM of tails and 85,111 MTHM of UNF have accumulated by 2050. Figure 5.10 shows the amount of fuel used in the EU. The tails mass accumulation rate is fairly steady, with peaks occurring when new reactors are deployed. In figure 5.11, the peaks are caused by reactor decommissioning which triggers all the batches in the final reactor core to be sent to the repository.

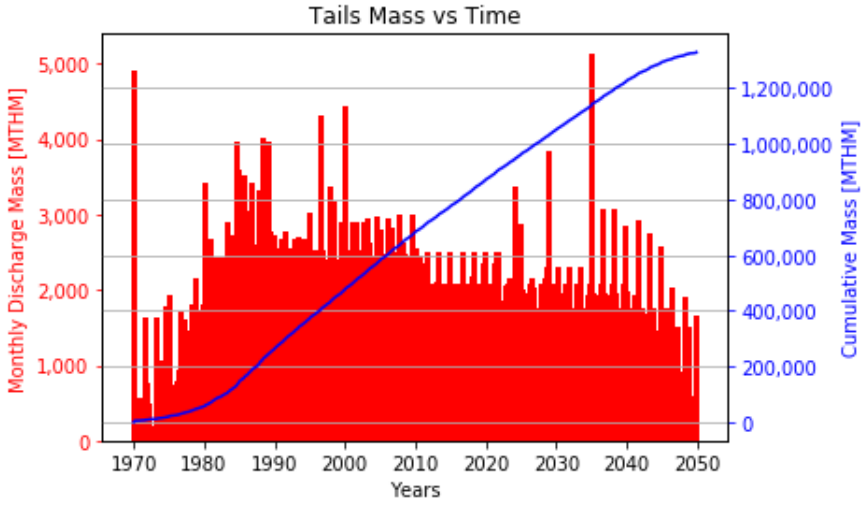

Figure 5.9: Simulated accumulation of tails in the EU is shown as a function of time.

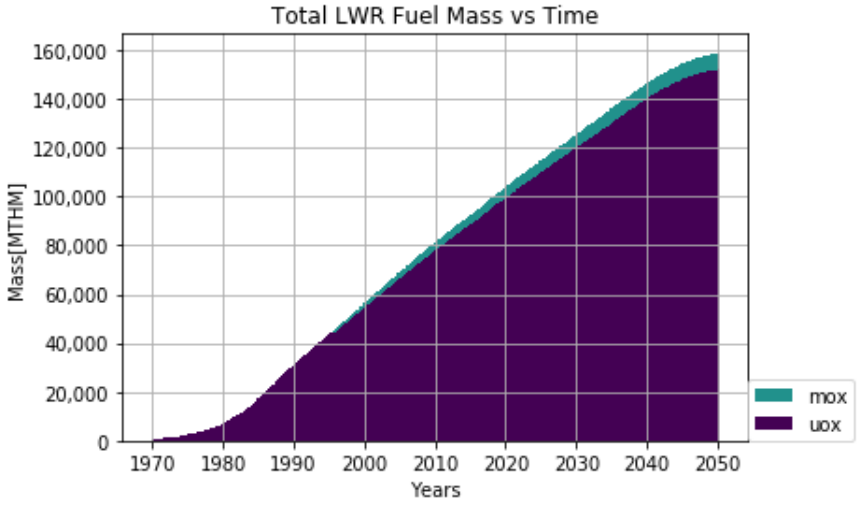

Figure 5.10: Simulated total EU fuel usage is shown as a function of time.

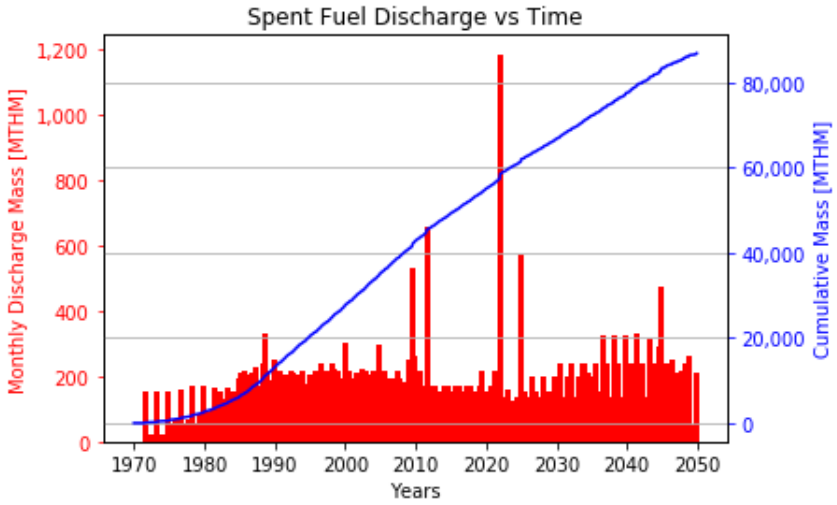

Figure 5.11: Simulated EU UNF accumulation and discharge is shown as a function of time. The large peak near 2025 is due to the planned German nuclear pahse-out, in which all German reactors will have been decommissioned by 2022.

French SFR deployment

Reprocessing the UNF collected from all EU nations can provide approximately 913 tons of plutonium. Table 5.7 lists the isotope, mass fraction, and quantity of plutonium that can be obtained from the 2050 UNF inventory. With the SFR breeding ratio above one, France can transition into a fully SFR fleet without extra construction of LWRs.

Table 5.7: Plutonium in the UNF inventory.

Isotope	**Mass Fraction in Used Fuel [%]**	**Quantity [t]**
Pu238	0.011	9.76
Pu239	0.518	506.05
Pu240	0.232	226.64
Pu241	0.126	123.09
Pu242	0.048	47.57
Total	0.935	913.14

From Varaine et al. [78], a French ASTRID-type 600MWe SFR consumes 1.125 metric tons of plutonium a year, with an initial plutonium loading of 4.9 metric tons.

Used MOX from an ASTRID reactor is 23.95% plutonium in this simulation (see table 7.1), whereas fresh MOX is 22% plutonium. The plutonium breeding ratio in this simulation is thus assumed to be ≈ 1.08.

Figure 5.12 shows MTHM of MOX loaded in the SFRs per month. The plot has peaks during a period of aggressive deployment of SFRs followed by an equilibrium at 83 MTHM. The peaks reoccur with the deployment of the second generation of SFRs. The spikes are due to initial fuel demand corresponding to these new deployments. The initial cores loaded into new SFRs rely on the MOX created from legacy UNF. Once the deployed SFRs create enough

extra plutonium, the legacy UNF is no longer used. Notably, this switch from a less preferred fuel origin to a more preferred fuel origin is handled automatically within CYCLUS via user-defined preferences within its dynamic resource exchange algorithm [27].

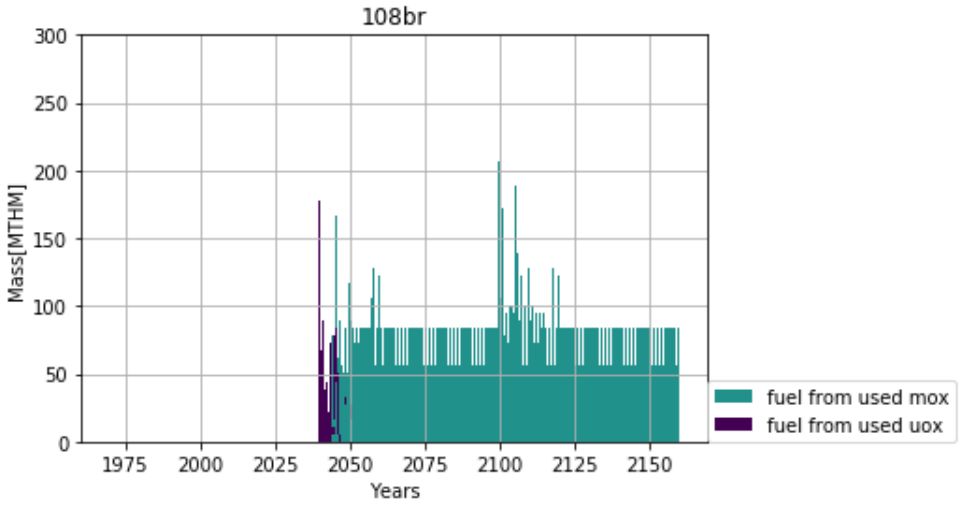

Figure 5.12: Fuel loaded into SFRs was simulated in discrete batches.

Figure 5.13 shows the separated plutonium discharge per month from the reprocessing plant. The plutonium outflux does not precisely follow the fuel demand because CYCLUS agents have material buffers that store commodity fuel for later usage. The reprocessed plutonium from legacy UNF is stored for the initial loading of SFRs. Plutonium separated from legacy UNF meets plutonium demans sufficiently to reduce the reprocessing demand for the first aggressive deployment of SFRs. The plutonium from reprocessing legacy fuel is a flat rectangle because the reprocessing throughput was set to 183.2 $\frac{MTHM}{month}$ to avoid reprocessing all the legacy in one timestep. This value is assuming that France doubles its current reprocessing capacity.

Table 5.8 lists French reprocessing and ASTRID fuel fabrication metrics.

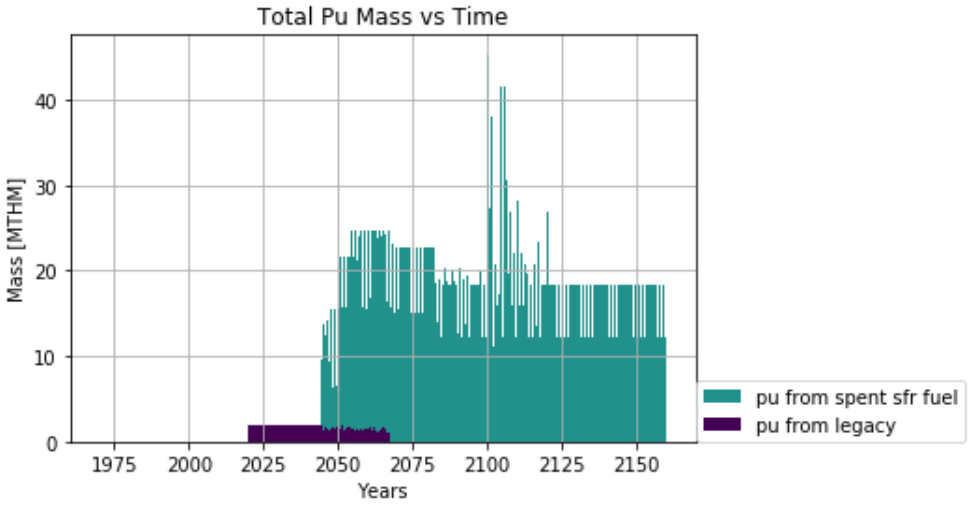

Figure 5.13: The separated plutonium discharge from the reprocessing plant in $\frac{\text{MTHM}}{\text{month}}$. The plutonium from LWR UNF is created after the demand is gone, due to material buffers in CYCLUS.

Table 5.8: In the French transition to SFRs, the total legacy UNF reprocessed is the amount of UNF France needs for a transition into a fully SFR fleet.

Category	**Unit**	**Value**
Total ASTRID MOX used	MTHM	62,144
Average UOX Reprocessing	MTHM/month	**144.29**
Average Total Reprocessing	MTHM/month	**61.3**
Average Fuel Fabrication	MTHM/month	**36.9**
Total SFRs Deployed		214
Total Plutonium Reprocessed	MTHM	13,671
Total ASTRID fuel from UOX Waste	MTHM	3,001
Total ASTRID fuel from MOX Waste	MTHM	59,143
Total Tails used	MTHM	48,472
Total legacy UNF reprocessed	MTHM	55,553
Total Reprocessed Uranium Stockpile	MTHM	194,186
Total Raffinate	MTHM	12,123

These results demonstrate that despite the large amount of initial plutonium that has to be reprocessed prior to ASTRID deployment, the 20 years (2020-2040) of ASTRID fuel preparation allows a reasonable level of average UOX reprocessing capacity demand.

5.8 Sensitivity analysis

I explored the impact of two key variables, the lifetime of French LWRs and the breeding ratio of ASTRID reactors. The range of these parameters (table 5.9) sought to capture the full span of their uncertainty.

Note that the breeding ratios of the ASTRIDs are artificially increased by editing the output fuel composition in the ASTRIDs. I did not take into account the other reactor parameters (e.g. core size, initial fuel composition, fuel residence time, etc.) that must be changed to achieve these higher breeding ratios. More detailed analyses of the reactor physics and their effect on this transition scenario are future work.

Table 5.9: Both LWR lifetime and ASTRID breeding ratio impact transitional reprocessing demand.

Parameter	**Default**	**Values**
Breeding Ratio of ASTRIDs	1.08	1.11, 1.15, 1.18
Lifetime of French LWRs [years]	60	65, 70, 80

5.8.1 Breeding Ratio

Increase in the breeding ratio of ASTRID reactors decreases the total reprocessing demand, since less UNF must be reprocessed to extract the same amount of plutonium. Additionally, ASTRIDs become independent more quickly due to higher breeding of plutonium.

Figure 5.14 shows the relationship between breeding ratio and fuel loading in ASTRIDs. The ASTRIDs produce more plutonium, reducing the plutonium demand from reprocessed UOX. However, since LWR UNF is not the limiting factor for this transition scenario, increasing the breeding ratio does not play a significant role in the transition scenario, especially considering the technical difficulty in achieving a high breeding ratio.

The sensitivity analysis also shows, as demonstrated in figure 5.15 that increasing the breeding ratio decreases the mass of LWR UNF required for the transition.

The differential impacts of varying the breeding ratios are shown in table 5.10. The differences were calculated using the following equation:

$$\epsilon = \frac{(x - x_{base})}{x_{base}} * 100$$

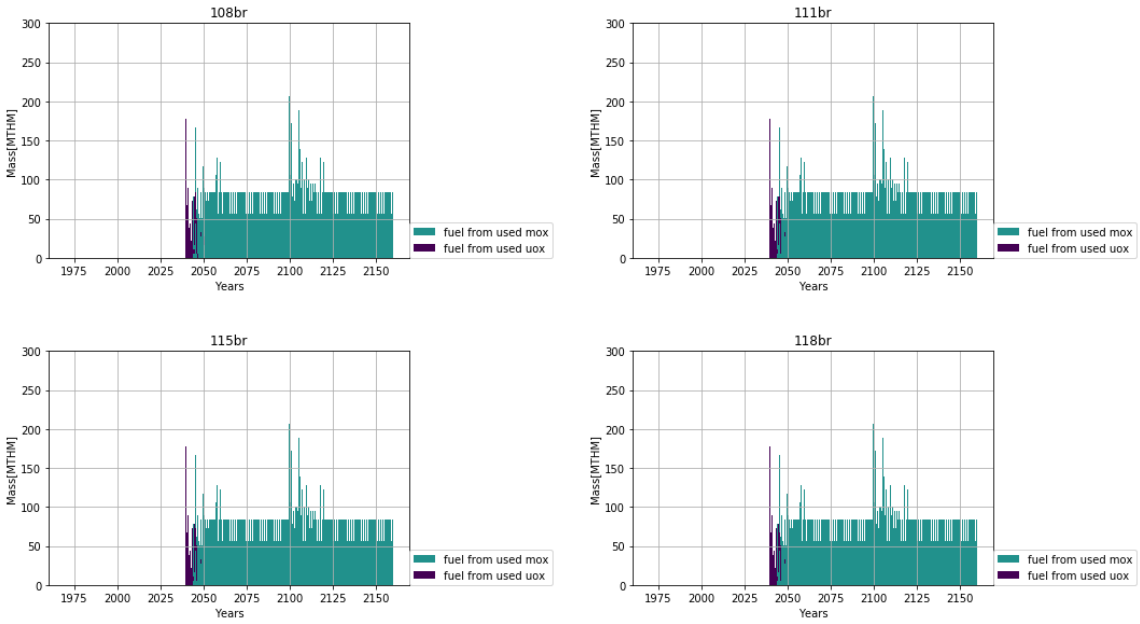

Figure 5.14: ASTRID fuel loading patters are altered by changes in ASTRID breeding ratio. Less ASTRID fuel comes from reprocessed LWR UNF because ASTRIDs generate more plutonium.

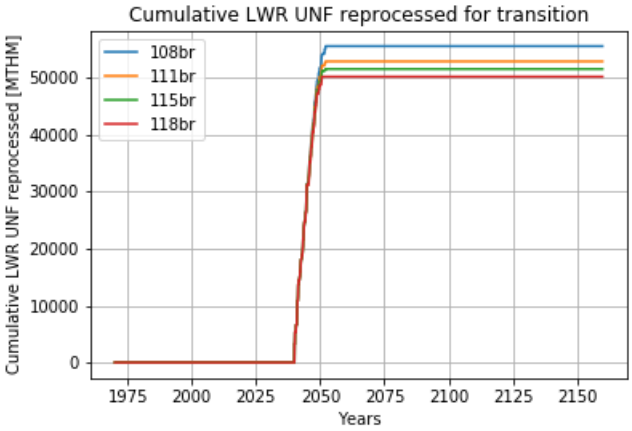

Figure 5.15: Sensitivity analysis demonstrates that increasing the breeding ratio decreases the required UOX UNF.

5.8.2 Lifetime Extension of French LWRs

Extending the lifetime of French LWRs lowers the average monthly UOX reprocessing demand, since the ASTRID deployment becomes delayed (shown in figure 5.16). The plutonium demand is delayed, allowing the reprocessing plant more time to prepare plutonium for ASTRID reactors.

Figure 5.17 shows the change in ASTRID fuel loading with LWR lifetime extension. The ASTRID fuel loaded with plutonium from LWR UNF conveys the corresponding LWR UNF reprocessing demand. The change in ASTRID

Table 5.10: Breeding ratio impact on reprocessing requirements.

	% Difference			
Breeding Ratio ⟶	**1.08**	**1.11**	**1.15**	**1.18**
Total reprocessing demand	0.0	-5.3	-7.8	-10.3
LWR UNF reprocessed	0.0	-4.8	-7.2	-9.6

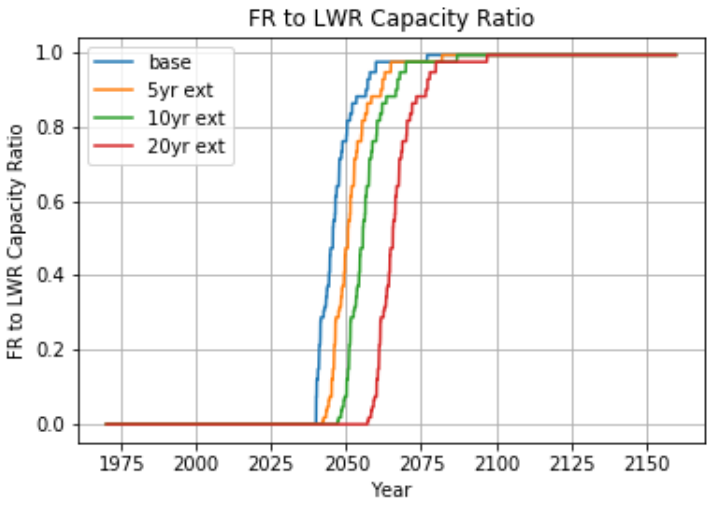

Figure 5.16: The ratio of ASTRIDs to LWRs in France demarcates the transition period.

deployment alters ASTRID fuel loading patterns. However, increasing the LWR lifetimes does not increase the LWR UNF demand significantly (less than 1% for the 20-year extension case), because ASTRIDs become self-sustaining at similar times after the first ASTRID deployment.

The quantitative effects of LWR lifetime extensions are shown in table 5.11. The differences were calculated using the same equation used for the breeding ratio study. Since LWR lifetime extensions shorten the span of ASTRID operations, less ASTRID fuel is needed when LWR lifetimes are extended. Therefore, it is not fair to compare the mass of total UNF reprocessed, since less plutonium is extracted from UNF. Instead, I compared the average reprocessing values and the total amount of LWR UNF reprocessed. There is not a significant difference (less than 1% for the 20-year extension case) in the amount of LWR UNF reprocessed. The delay in ASTRID deployment spreads out the LWR UNF reprocessing demand, thereby dramatically reducing (39% for the 20-year extension case) the average monthly LWR UNF reprocessing demand.

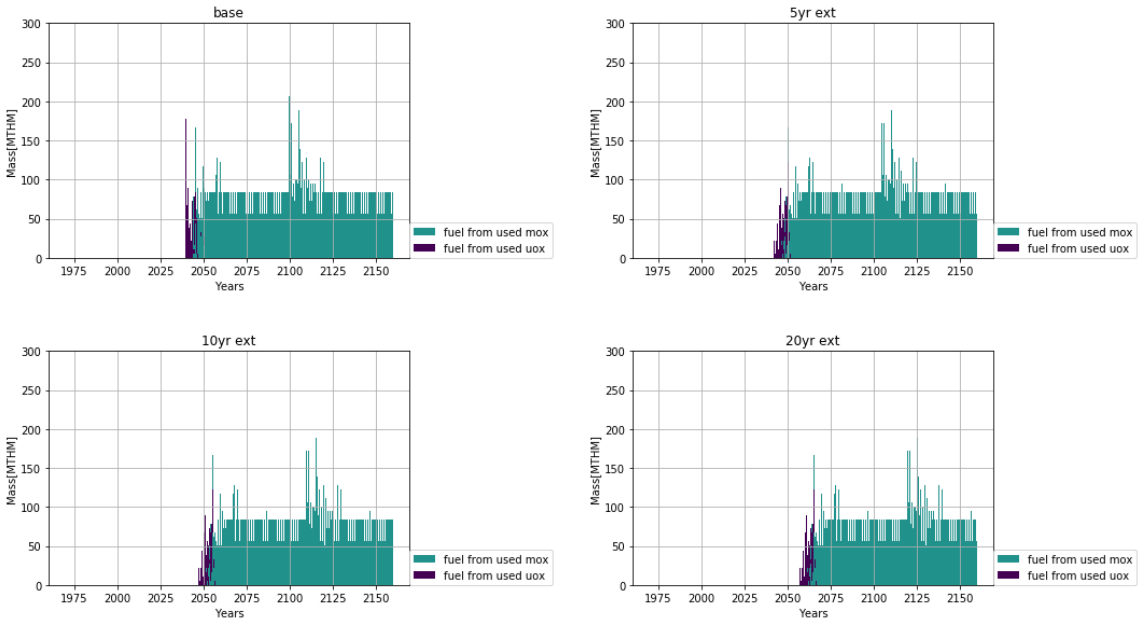

Figure 5.17: ASTRID fuel loading patterns are altered by changes in ASTRID deployment caused by the lifetime extension of LWRs.

Table 5.11: LWR lifetime extension impact on reprocessing requirements.

	% Difference			
LWR lifetime extension ⟶	**0 years**	**5 years**	**10 years**	**20 years**
Total ASTRID fuel produced	0.0	-3.9	-8.0	-16.3
LWR UNF reprocessed	0.0	-0.7	-0.7	-0.7
Average LWR UNF reprocessed	0.0	-16.0	-25.7	-39.8
Average UNF reprocessed	0.0	-2.3	-4.2	-8.3

5.9 Conclusion

France can transition into a fully SFR fleet with installed capacity of 64,700 MWe without building additional LWRs if France receives UNF from other EU nations. Supporting the SFR fleet requires an average reprocessing capacity of 61.3 MTHM per month, and an average fabrication capacity of 36.9 MTHM per month.

The sensitivity study explored the effect of increased SFR breeding ratio and existing LWR lifetime extension. Increasing the breeding ratio reduced the amount of LWR UNF required to transition up to 9.6% and decreased the total reprocessing demand up to 10.3%. Increasing the lifetime of existing LWRs was not significant in reducing the LWR UNF required to transition, but provided the benefit of decreased average reprocessing demand due to delayed ASTRID transition.

Since most EU nations do not have an operating UNF repository or a management plan, they have a strong incentive to send their UNF to France. In particular, the nations planning aggressive nuclear reduction will be able

phase out nuclear without constructing a permanent repository. France has an incentive to take this fuel, since recycling used fuel from other nations will allow France to meet their MOX demand without new construction of LWRs.

Table 5.12 lists EU nations and their UNF inventory in 2050. I analyzed a strategy in which the nations reducing their nuclear fleet send their UNF to France. The sum of UNF from Bulgaria, Poland, Czech Republic, Italy, Slovenia, Belgium, Spain and Germany provides enough UNF for the simulated transition ($\approx 55,500$ MTHM). These nations are shown in bold in table 5.12. Sweden and Finland are not considered because they have established national nuclear waste management plans.

If France receives LWR UNF from all EU nations, except Sweden and Finland, it will have a surplus of 20,516 MTHM of LWR UNF. This inventory can be leveraged to increase nuclear power capacity as the transition takes place. However, pragmatic limitations such as new reactor construction, reprocessing throughput, and political concerns remain.

Table 5.12: EU nations and their respective UNF inventory.

Nation	Growth Trajectory	UNF in 2050 [MTHM]
Poland	**Aggressive Growth**	**1,807**
Hungary	Aggressive Growth	3,119
UK	Aggressive Growth	13,157
Slovakia	Modest Growth	2,744
Bulgaria	**Modest Growth**	**2,965**
Czech Rep.	**Modest Growth**	**4,143**
Finland	Modest Growth	5,604
Netherlands	Modest Reduction	539
Italy	**Modest Reduction**	**577**
Slovenia	**Modest Reduction**	**765**
Lithuania	Modest Reduction	1,051
Romania [1]	Modest Growth	7,495
Belgium	**Aggressive Reduction**	**4,799**
Spain	**Modest Reduction**	**9,725**
France	**Modest Reduction**	**12,582**
Sweden	Aggressive Reduction	16,014
Germany	**Aggressive Reduction**	**18,096**

[1] Romania only has PHWRs. The used PHWR fuels are not considered for reprocessing.

On the other hand, in these simulations, some complex political and economic factors were not incorporated and various assumptions were present in this scenario. For example, Germany's current policy is to not reprocess its LWR fuel [76], and this policy would create a shortage in the supply of LWR UNF for ASTRID MOX production. Continuation of that German policy would not, however, be incompatible with a change in EU policy that frees EU countries from creating their high level waste repositories, since France could still agree to take in Germany's UNF for direct disposal. The analysis method described herein could readily be adapted to account for such possibilities.

The collaborative option explored here may hold value for the EU nuclear community, and may enable France to advance more rapidly into a closed fuel cycle.

Chapter 6

United States NFC transition scenario into an MSR fleet

nuThe United States has been the forerunner in nuclear energy, with a currently installed nuclear capacity of 99,221 MWe [41]. With its large capacity and long history of nuclear energy, the United States has accumulated over 70,000 MTHM of UNF.

The challenge with modeling the U.S. transition scenario is that the U.S. does not have a single nationwide advanced reactor vision, whereas France has a central plan to transition into ASTRID reactors [11, 78]. Previous analyses of the United States [82, 71] NFC transition scenario assumed transition to fast-spectrum SFRs. However, the fact that the U.S. nuclear reactor fleet is decided by economic interests (industries), necessitates exploration of different options, such as transitioning into MSRs.

As explained in section 1.4.2, rising interests in MSR designs led to a proliferation of U.S. corporations aiming to commercialize MSR designs. Given the large interest from industries, MSR designs may someday be commercially deployed in the United States.

In this chapter, I explore the U.S. transition scenario from an LWR fleet into an MSR fleet.

6.1 Initial conditions and scenario parameters

For the French scenario, the UNF inventory at the present time is calculated by simulating the nuclear operational history from 1970. However, this is unnecessary for the U.S. scenario because a detailed database exists that describes the U.S. UNF inventory up to May of 2013. The Used Nuclear Fuel Storage Transportation and Disposal Analysis Resource and Data System (UNF-ST&DARDS) is a comprehensive, controlled source of UNF information, including dry cask attributes, assembly data, and economic attributes [58]. The assembly compositions are calculated using ORIGEN [56] using the reported fuel assembly burnups, original enrichment, and assembly design. This database allows the transition scenario simulation to start from 2013. I imported the UNF inventory mass and composition in 2013 from UNF-ST&DARDS and 'initiated' the inventory in the simulation as a `Source` facility with an inventory of 68,072 MTHM, the total mass of the LWR UNF in the UNF-ST&DARDS.

Furthermore, the U.S. currently has additional uranium resources in the form of more than 700,000 MTHM

of depleted uranium [55], which is a waste product of enrichment. The depleted uranium inventory is currently a liability and waste, but can be utilized as fertile material in a U-Pu fuel cycle. If the U.S. chooses a Th-^{233}U fuel cycle, additional thorium resources are needed, while with a U-Pu cycle, the U.S. can use its waste to create fuel.

The U.S. nuclear fleet in 2013 can be extracted from the PRIS database. The same assumption that legacy reactors have a 60-year lifetime is applied to calculate the remaining lifetime of legacy reactors. I used `from_pris` to generate the expected power capacity of the current U.S. nuclear from 2013 (shown in figure 6.1).

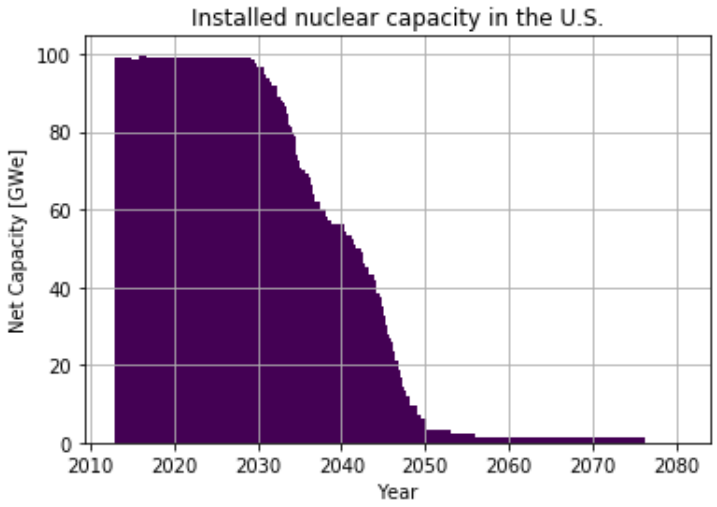

Figure 6.1: Installed nuclear capacity in the United States from 2013.

6.1.1 Energy demand prediction

A reference for the energy demand prediction is the U.S. Energy Information Administration (EIA) Annual Energy Outlook [19]. The 2018 Annual Energy Outlook report predicts an annual electricity demand growth of 0.9%. The report also predicts that nuclear power will either remain static or decrease. The report predicts that nuclear capacity will decrease from 99 GWe to 79GWe in 2050, with no new plants beyond 2020. However, for this work, I assume that the U.S. nuclear power capacity is kept at 100GWe, and new reactors are deployed to make up for the decommissioned capacity.

6.1.2 MSR design and availability

MSR designs can be categorized depending on their operating neutron spectrum (e.g. fast, thermal), fuel cycle (e.g. Th-^{233}U, U-Pu), and transmutation goals (e.g. breeder, burner). Selection of an MSR design depends on factors like economics, safety, and fuel cycle considerations. For this work, I choose a fast, U-Pu cycle, burner MSR design

named REBUS-3700 [53] to deploy for the transition analysis.

The REBUS-3700 MSR design offers five principal advantages over other MSR designs:

- Fast spectrum - no need for moderator rods
- U-Pu cycle - requires only depleted uranium for supply after initial fuel salt loading
- Weakly positive breeding gain (0.03)
  - Self-sufficient (no external fissile input)
  - No surplus fissile material production (stabilizes Pu inventory)
- U-TRU initial fuel - transmutation of long-lived actinides
- Simpler design - no radial / axial blanket

The U.S. has a large inventory of LWR UNF and tails. The benefits of the REBUS-3700 design aligns with the waste management interest of the U.S. Reducing final geological repository burden can be accomplished by:

- Reduction of TRU inventory by transmutation in the reactor (table 6.1)
  - Reduction of long-term decay heat and activity (figure 1.1)
  - More 'tailored' waste form design for fission products
- Reducing tails inventory

Additionally, the REBUS-3700 does not have, at any moment in operation, separated fissile streams, like other MSR designs. Other MSR designs such as the Molten Chloride Salt Fast Reactor (MCSFR) design [69] have separated fissile streams, since it separates the bred plutonium from its blanket salt. The REBUS-3700 only takes in depleted uranium and processes out fission product groups such as volatile gases and noble metals. The detailed reprocessing scheme is shown in table 6.2. This self-sustained and closed operation increases its non-proliferation properties.

The initial fuel and equilibrium TRU isotopic composition of REBUS-3700 is shown in table 6.1. The TRU isotopic composition matches that of the LWR UNF after 8.5 years of decay (shown in figure 6.2).

6.2 U.S. deployment schedule

As shown in figure 6.1, the U.S. will undergo a profound loss of nuclear capacity from 2030, under the assumption that U.S. reactors have a lifetime of 60 years.

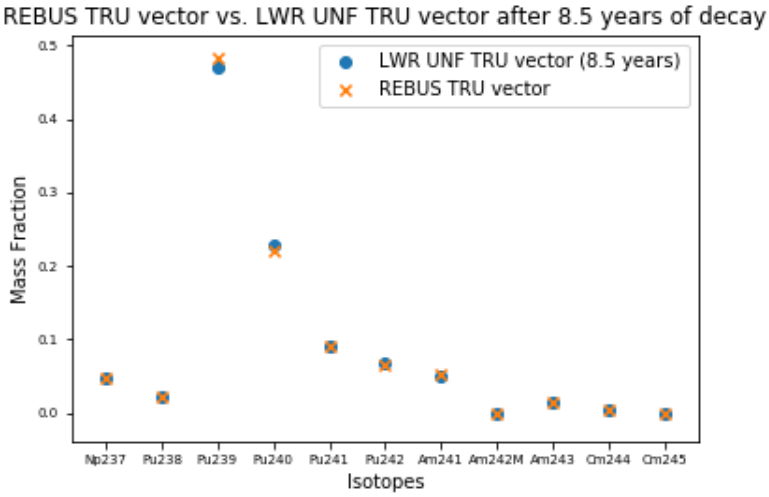

Figure 6.2: TRU vector of REBUS-3700 initial fuel from Mourogov et al. [53] with LWR UNF after 51 GWdth/MTHM burnup and 8.5 years of decay

Table 6.1: Initial and equilibrium TRU isotopic composition from Mourogov et al. [53].

Isotope	Beginning of Life	Equilibrium (~6500 EFPD)
^{237}Np / ^{239}Np	4.80 / 0.00	0.65 / 0.07
^{238}Pu / ^{239}Pu	2.13 / 48.33	2.23 / 58.02
^{240}Pu / ^{241}Pu / ^{242}Pu	22.17 / 9.05 / 6.38	27.63 / 3.35 / 4.05
^{241}Am / ^{242m}Am / ^{243}Am	5.17 / 0.01 / 1.48	1.50 / 0.12 / 1.05
^{242}Cm / ^{243}Cm	0.0 /0.0	0.07 / 0.01
^{244}Cm / ^{245}Cm / ^{246}Cm	0.43 / 0.04 / 0.00	1.02 / 0.19 / 0.05
Equivalent enrichment, %	10.1	11.0
TRU fraction in heavy atoms, %	15.6	15.9

Since it is unlikely that MSRs are ready for commercial deployment in 2020, I deploy LWRs (AP 1000 design [72]) to make up for the decommissioned capacity in the simulation. After 2050, REBUS-3700 design MSRs are deployed. The deployment of new reactors is shown in figure 6.4, and the installed power capacity of the reactors is shown in 6.3. In the simulation, 84 additional LWRs and 95 MSRs are deployed.

6.3 Material flow

The fuel cycle is represented by a series of facility agents whose material flow is illustrated in figure 6.5, along with the CYCLUS archetypes that were used to model each facility.

The U.S. transition scenario's material flow is similar to that of the French transition in the previous chapter, except that all TRU is reprocessed from LWR UNF to fabricate fuel salt. Also, the depleted uranium from the enrichment plant is stored in a storage facility to be used as a fertile stream for MSR facilities. Natural uranium is

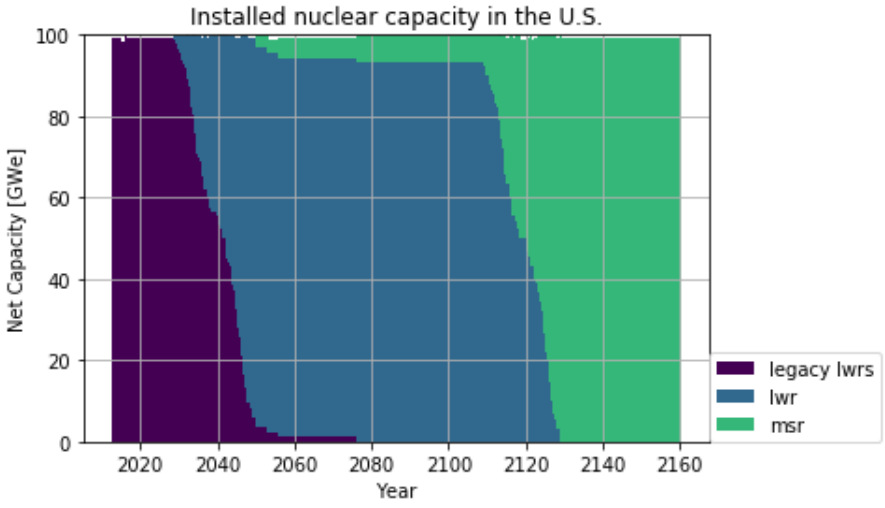

Figure 6.3: Power capacity separated by reactor type from 2020.

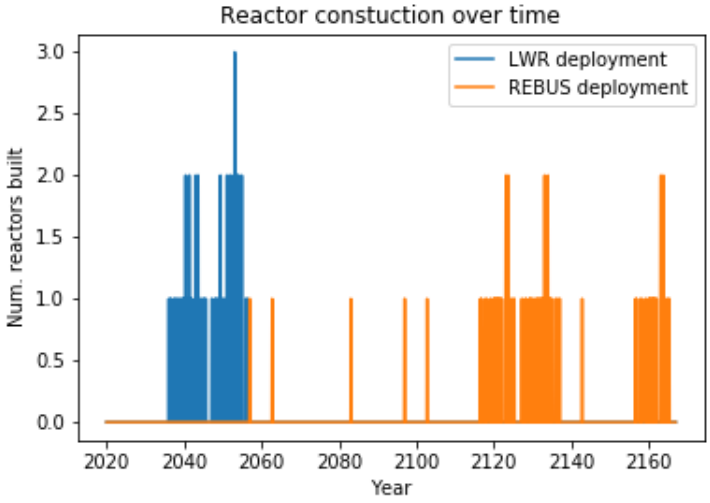

Figure 6.4: New reactor deployment from 2020.

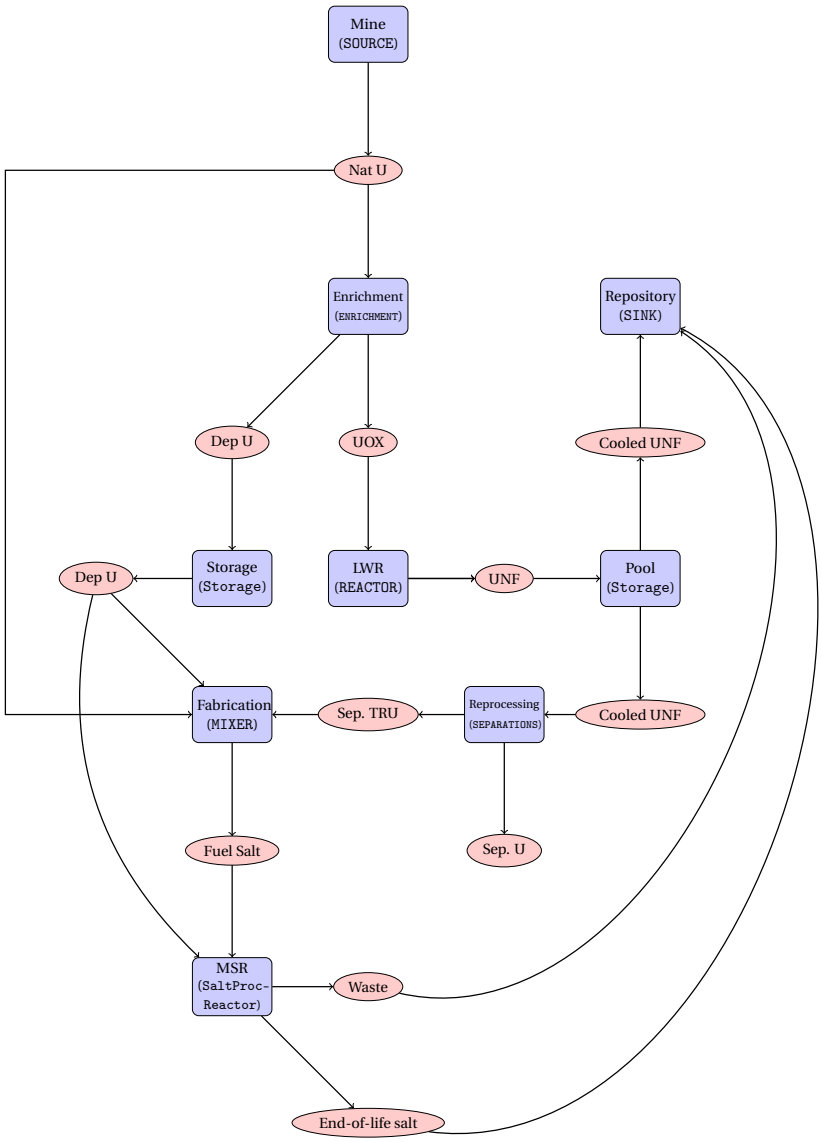

Figure 6.5: Fuel cycle facilities (blue boxes) represented by CYCLUS archetypes (in parentheses) pass materials (red ovals) around the simulation.

Table 6.2: Reprocessing scheme for REBUS-3700

Group	Elements	Reprocessing Time (s)
Volatile Gases	Kr, Xe, Ar, Ne, H, N, O, Rn	30
Noble Metals	Se, Nb, Mo, Tc, Ru, Rh, Pd, Ag, Sb, Te, Zr, Cd, In, Sn	30
Rare Earths	Y, La, Ce, Pr, Nd, Pm, Sm, Gd, Eu, Dy, Ho, Er, Tb, Ga, Ge, As, Zn	259,200

mixed with the reprocessed TRU to create fuel salt. Lastly, instead of a single stream of MOX UNF from the MOX reactors, MSRs output two streams - reprocess waste and end-of-life salt - which are both disposed.

6.4 Scenario specification

The scenario specifications for the U.S. transition scenario are listed in table 6.3. The simulation end date is set to 2160 so that second generation of large MSR deployment is included in the simulation. MSR fuel production begins 20 years prior to MSR deployment to reduce reprocessing and fabrication burden. LWR UNF is cooled for a minimum of 8.5 years so that the TRU vector is similar to the TRU vector of REBUS-3700 initial fuel (see figure 6.2). The reprocessing plant separates all TRU, and mixes the separated TRU elements into MSR fuel.

Table 6.3: Simulation Specifications

Specification	**Value**	**Units**
Simulation Starts	2013	year
Simulation Ends	2160	year
Production of MSR fuel begins	2030	year
MSRs become available	2050	year
Reprocessed uranium usage	None	-
Minimum UNF cooling time	8.5	years
Separation efficiency of TRU and U	99.8	%
Reprocessing streams	Am, Pu, Cm, Np and U	-
Reprocessing capacity	∞	MTHM/month
MSR fuel salt fabrication throughput	No limit (∞)	MTHM/month

6.5 Reactor specifications

Two major reactors are used in the simulation, PWR and MSR. For PWRs, I use a linear core size model to capture varying reactor capacity (explained in section 3.1). The reactors deployed after 2020 are modeled after the AP-1000 reactor [72], and I assume a PWR lifetime of 80 years. The reactor specifications are shown in 6.4. The MSR does not have a refueling outage and runs continuously.

Table 6.4: Baseline LWR and MSR simulation specifications.

Specification	**PWR [72]**	**MSR [53]**
Lifetime [y]	80	40
Cycle Time [mos.]	18	continuous
Refueling Outage [mos.]	2	N/A
Rated Power [MWe]	1110	1628
Assembly mass [kg]	446	N/A
Batch mass [kg]	23,192	N/A
Core mass [kg]	70,022	200,100
Discharge Burnup [GWd/tHM]	51	N/A
Assemblies per core	157	N/A
Batches per core	3	N/A
Initial Fissile Loading [t]	3.1 ^{235}U	19.13 TRU
Fuel	UOX	TRU-U Cl Salt

6.6 Material definitions

Depletion calculations for the LWR nuclear fuel are recipe-based, such that a fresh and used fuel recipe is calculated beforehand using ORIGEN (see table 7.1). ORIGEN calculates buildup, decay, and processing of radioactive materials [56]. This recipe has also been used for repository performance modeling [81]. For fresh LWR fuel, I assume a fuel enrichment of 3.1% U235.

For depletion calculations of MSR fuel, I use SaltProc (section 2.2) to obtain depleted fuel compositions and waste stream composition in a continuously reprocessing reactor. The initial composition used in this simulation for the REBUS-3700 reactor is shown in table 6.5.

Table 6.5: Initial fuel salt composition for REBUS-3700

Isotope	**Mass %**
Na23	6.752
Cl35	26.753
Cl37	9.227
U235	0.343
U238	47.362
Np237	0.459
Pu238	0.204
Pu239	4.623
Pu240	2.12
Pu241	0.866
Pu242	0.61
Am241	0.494
Am243	0.142
Cm244	0.041
Cm245	0.004

6.7 Database generation

The database used to model MSRs is generated using SaltProc with a unit cell model of the REBUS-3700 reactor. The parameters used for running SERPENT and SaltProc are shown in table 6.6. The parameters were chosen to acquire a reasonably accurate simulation result while keeping the simulation time under 48 hours. I chose SERPENT simulation parameters so that the eigenvalue (k_{eff}) uncertainties for any SERPENT run does not exceed 42 ppm. The fuel salt density and power density was obtained from values in the literature [53]. I derived the fuel salt mass by dividing the core fuel mass by the core volume.

$$\rho_{fuel} = \frac{M_{core}}{V_{core}} = \frac{133.3t}{368,587l} = 3.6\frac{g}{cm^3}$$

I set SaltProc simulation parameters to keep the number of SERPENT 3-day depletion calculations under 800.

Table 6.6: SaltProc simulation parameters used to generate the database for REBUS-3700

Parameter	**Value**
SERPENT Parameters	
Num. neutrons per generation	8,000
Num. active generation	150
Num. inactive generation	50
Burnup calc. mode	CRAM
Power density	$32.18e-3\ \frac{kW}{g}$
Depletion step	30 days
Fuel salt density	$3.6\frac{g}{cm^3}$
SaltProc Parameters	
Lifetime [y]	60
Total timesteps	730
Reprocessing Scheme	As table 6.2
Refill material	Depleted uranium (0.3% ^{235}U)

The change in K_{eff} values in the REBUS-3700 core during its lifetime is shown in figure 6.6. A lifetime of 40 years is set for the REBUS-3700 reactor since the k_{eff} value drops below 1.01 after 40 years of operation, according to the SaltProc results. The REBUS reactor discharges waste (reprocessed elements - in table 6.2) at an average rate of $90.34\frac{kg}{month}$ (figure 6.7).

This database is generated to demonstrate MSR modeling capability in CYCLUS, and there is a possibility for future benchmarking if other simulation tools are applied to the topic.

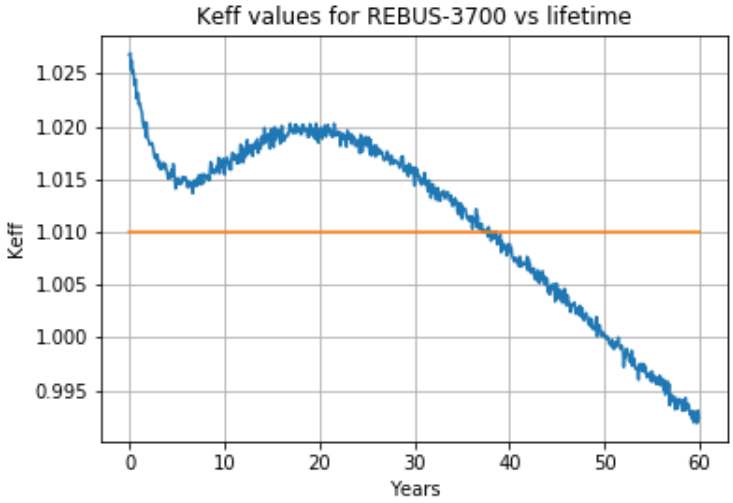

Figure 6.6: Change in k_{eff} value in the REBUS-3700 core. The k_{eff} drops below 1.01 after 40 years of operation.

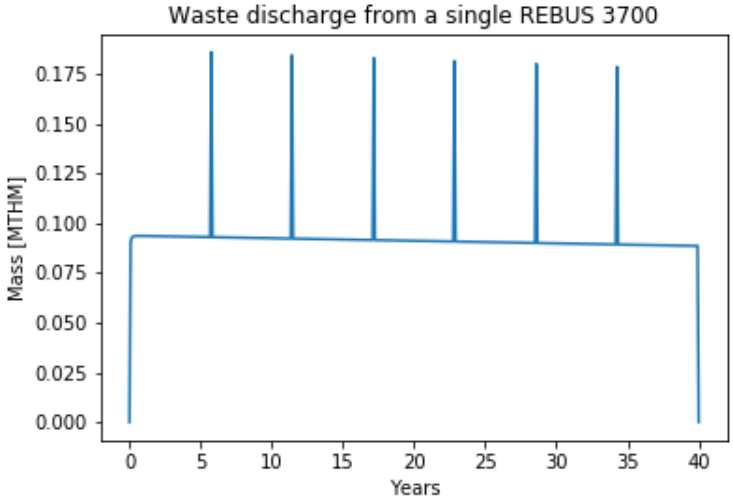

Figure 6.7: Mass of waste discharged from a single REBUS reactor. The peaks are due to the timestep differences in CYCLUS and SaltProc. CYCLUS uses 30.43 days for a month (1/12 of 365.25), and SaltProc uses 30-day timesteps. The peaks occur when two SaltProc timestep-worth of waste is discharged per one CYCLUS timestep.

6.8 Results

Results show that the United States can transition into a fully MSR fleet, while reducing final repository burden by reducing TRU and depleted uranium inventory.

6.8.1 LWR UNF inventory

Table 6.7 lists the U.S. LWR UNF inventory results in the simulation. Since major deployment of MSRs does not begin until 2110, the U.S. has a long time to prepare and accumulate the TRUs required for MSR fuel salt fabrication. The U.S. accumulates an additional 196,976 MTHM of LWR UNF from 2013 to 2130, the year when the last LWR decommissions. Figure 6.8 shows the accumulation of LWR UNF. This figure does not subtract the LWR UNF reprocessed.

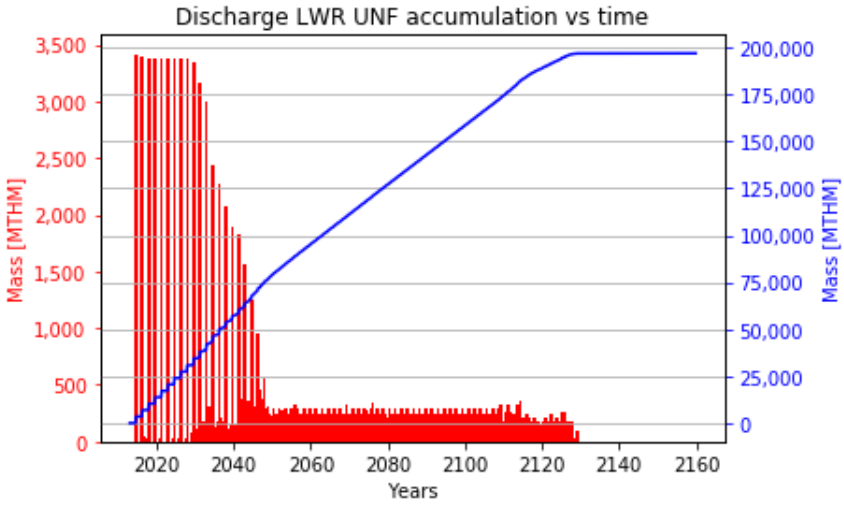

Figure 6.8: The cumulative mass of U.S. LWR UNF. The red bars are the mass discharged per timestep, and the blue line is the cumulative inventory. The large discharge quantity prior to 2040 is because the legacy LWRs are deployed in the first timestep, thus discharging their fuel in sync. The later deployed LWRs are not in sync, which makes the monthly discharge values more averaged out.

Table 6.7: U.S. LWR UNF material flow and inventory

Category	**Value [MTHM]**
US UNF UOX generated in 2013-2050	78,281
US legacy LWR UNF in 2013	68,072
Total US LWR UNF inventory in 2050	146,353
Total US LWR UNF created from 2013	196,976
Total US LWR UNF created in U.S.	265,048

6.8.2 Reprocessing and fabrication material flow

Metrics for LWR UNF reprocessing are shown in table 6.8. A total of 19,015 MTHM of fuel salt is sent to MSRs. A total of 134,927 MTHM of LWR UNF are reprocessed to extract the TRU for the fuel.

Figure 6.9 shows the cumulative quantity of LWR UNF reprocessed over time. The initial stage (2050-2100) is characterized by a small amount of reprocessing due to the small number of MSRs deployed. From 2100, aggressive deployment of MSRs causes a large increase in the amount of LWR UNF reprocessed. This sudden jump in demand of fuel salt is mediated by reprocessing the LWR UNF beforehand.

Table 6.8: U.S. reprocessing metrics

Category	**Value [MTHM]**
Total fuel salt mass sent to MSRs	19,015
Total TRU extracted from LWR UNF	1,815
Total LWR UNF reprocessed	134,927
Average monthly reprocessing demand of LWR UNF	94.15
Average monthly fabrication of fuel salt	13.26
Total raffinate stockpile	4,024

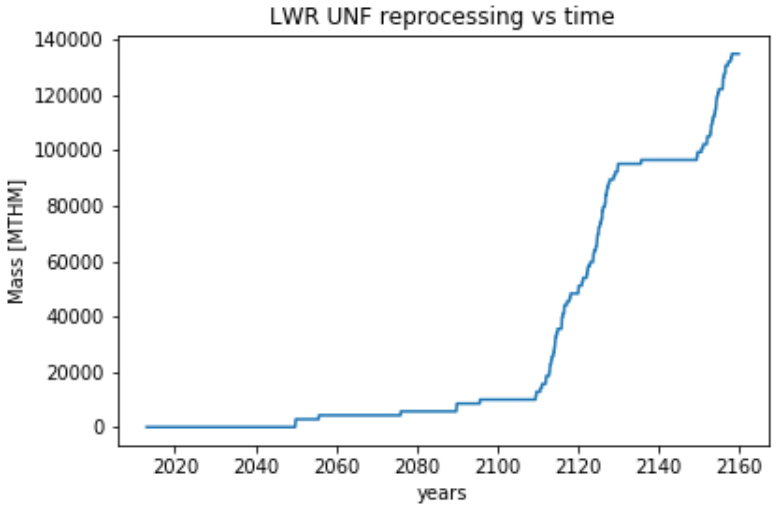

Figure 6.9: The Cumulative mass of LWR UNF reprocessed for MSR salt fabrication.

6.8.3 Waste inventory and resource usage

Table 6.9 shows the masses of various nuclear waste inventories at the end of the simulation. Large quantities of LWR UNF (132,094 MTHM) and depleted uranium (1.1 million tons) remain unused, meaning that more MSRs could have been deployed. The tails usage from the MSRs is not significant compared to the quantity of tails accumulated

(0.2% of the total tails inventory). One way to use more tails is to substitute depleted uranium for initial fuel salt fabrication. This would mean increasing the TRU composition in the fuel salt to make up for the decrease in ^{235}U, which is viable, since there are still 132,094 MTHM of LWR UNF leftover to extract TRU from.

Figure 6.10 shows the monthly discharge and cumulative inventory of waste from MSRs. The discharge mass increases with MSR deployment. The mass of depleted uranium sent to MSRs coincides with the waste outflux, since the mass in the MSR is kept constant.

Table 6.9: U.S. waste metrics.

Category	**Value [MTHM]**
LWR UNF leftover inventory	130,120
Total waste from MSRs	2,972
Total tails created from 2013	1,192,722
Total reprocessed uranium stockpile	260,867
Total tails used	2,972
Total remaining tails inventory	1,189,753
Total natural U used	1,389,698

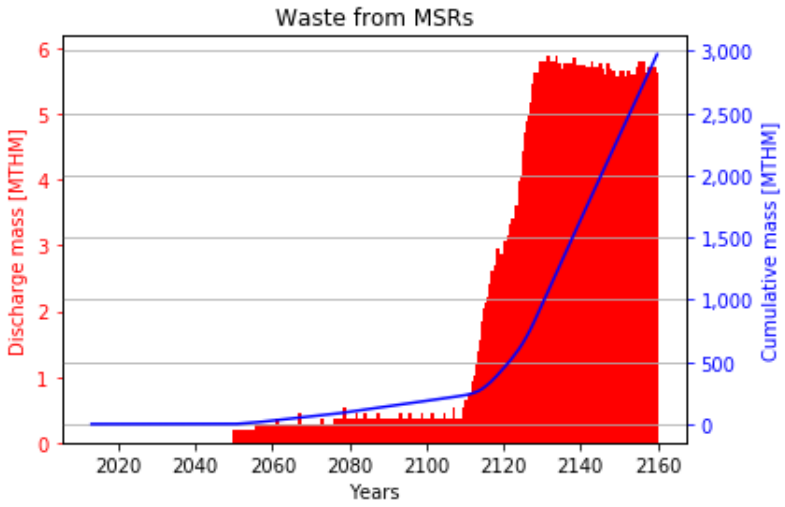

Figure 6.10: Monthly discharged waste and cumulative waste inventory from MSRs. The red bars are monthly discharge values, while the blue line is the cumulative quantity.

6.9 Conclusion

The United States can transition into a fully MSR fleet with an installed capacity of 100 GWe by 2130. With the deployment scheme used in the simulation, the U.S. will have sufficient time to prepare the fuel salt necessary for major MSR deployment beginning in 2110. Supporting the MSR fleet requires an average LWR UNF reprocessing

capacity of 94.15 MTHM per month, and an average fuel salt fabrication capacity of 13.26 MTHM per month. The reprocessing capacity demand is similar to the current capacity of the La Hague plant in France (91.6 MTHM per month) [65].

The deployment of the REBUS-3700 MSR design allows a reduction in final repository burden, by transmuting the TRU and reducing depleted uranium inventory. However, TRU extraction requires more advanced reprocessing methods than the currently widely-deployed PUREX method. Resource utilization can be improved if depleted uranium is used instead of natural uranium to fabricate initial fuel, since there is still more than one million tons of depleted uranium available at the end of the simulation. This would require a higher TRU concentration in the fuel, which is plausible since 132,094 MTHM of LWR UNF are still available for reprocessing.

In reality, however, complications with TRU vectors and changes in MSR performance will occur, due to variations in LWR UNF cooling (decay) time and discharge burnup. This would require careful fabrication of the initial fuel salt so that the desired reactor parameters - multiplication factor, power density - are achieved. Another challenge of this transition scenario is the aggressive build rates, which is not considered in this work.

In conclusion, the U.S. can reduce its waste inventory by transitioning into burner MSRs. Choosing a U-Pu cycle instead of a Th-^{233}U cycle eliminates the need to introduce new resources (thorium), usage of moderators, and allows utilization of depleted uranium, which would otherwise be waste. Fissile (separated TRU) and fertile (depleted uranium) material are not limiting factors in the simulation, and a large inventory of LWR UNF and depleted uranium remained at the end of the simulation.

Chapter 7

Conclusion and future work

This thesis expands and demonstrates the capabilities of CYCLUS, the agent-based fuel cycle simulator, to model real-world nuclear fuel cycle transition scenarios. CYCLUS has a novel framework that is modular and expandable, that allows addition of functionalities without editing CYCLUS itself.

I developed `cyclus_input_gen` to integrate historical nuclear operations by generating a CYCLUS input file from a PRIS database. I also developed an MSR module in CYCLUS that uses a database generated by a high-fidelity MSR simulation to model MSRs in a large fuel cycle simulation. The two added capabilities leverage CYCLUS' existing capabilities to model complex, real-world nuclear fuel cycle transition scenarios.

I compared CYCLUS' results with the results from other fuel cycle simulators (DYMOND [83], VISION [43], ORION [28], and MARKAL [68]) for a generic NFC transition scenario from an LWR fleet to an SFR fleet. Results show excellent agreement, except for disagreement caused by differences in reactor depletion behavior at the end of reactor lifetime, and whether fuel discharge is discrete or continuous. The CYCLUS simulation's SFR core size was 1.08% because CYCLUS can only have integer number batches, while the benchmark had 3.96 batches, which is unrealistic. This difference causes the unused TRU inventory in the CYCLUS simulation to be smaller initially, since more TRU is used for the initial loading of the SFR cores.

I simulated the French NFC transition simulation scenario to demonstrate Cyclus' capacity to model the historical nuclear operation of multiple regions. It also showed that France can transition from its LWR fleet into a fully SFR fleet without additional construction of LWRs if France receives LWR UNF from other EU nations.

I simulated the U.S. NFC transition simulation scenario to demonstrate Cyclus' capacity to roughly model MSRs in a large NFC simulation. The simulation showed that the U.S. can transition into a fully MSR fleet, and that availability of nuclear materials (LWR UNF and depleted uranium) is not a constraint.

7.1 Future work

Continued research into better methods of modeling fuel cycle transition scenarios and fuel cycle facilities can progress in multiple directions.

First, efforts can be made to incorporate uncertainties in future fuel cycle simulations by enabling CYCLUS to accept statistical distribution and symbolic functions as input parameters. Parameters such as LWR fuel burnup and enrichment evolve in time and can be better modeled by a function of time than a static parameter. Similarly, reactor parameters such as refueling time and cycle time can be better described by sampling from a distribution (e.g. gaussian) rather than the current static value.

Second, implementing reactor archetypes that directly preform depletion calculations could increase material inventory accuracy. The reactor archetypes used in this work use spent fuel recipes depleted outside of CYCLUS by higher fidelity tools, meaning that there are no depletion calculations performed by CYCLUS during runtime. While using a recipe to obtain depleted fuel composition is quick, it does not take into account the variations in input fuel composition. Unfortunately, conducting unique depletion calculations for each reactor discharge represents a significant computational burden. Additionally, imprecision introduced through simplifying assumptions inherent in fuel cycle modeling (e.g. deployment schedules, separation efficiency, constant reactor cycle time) significantly impact fuel cycle metrics. These effects typically dwarf precision improvements that higher fidelity depletion modeling might enable.

7.2 Closing remarks

The ANS chose closing the NFC as one of its grand challenges. ANS defined the challenge to be solved by firmly establishing the pathway that leads to closing the nuclear fuel cycle to support the demonstration and deployment of advanced fission reactors, accelerators, and material recycling technologies to obtain maximum value while minimizing environmental impact from using nuclear fuel. The research and development of such technologies need to be deliberate. NFC transition scenario simulation and analysis is the first step in identifying technological needs and goals. The identified technological needs will drive national policy and R&D funding. As demonstrated by this thesis, CYCLUS, with its modular structure and expandable nature, is essential in that effort.

7.3 Fresh and Used Fuel Composition

Isotope	Used ASTRID Fuel	Used UOX Fuel	Used MOX Fuel
He4	8.2631E-05	9.4745E-07	2.5108E-05
Ra226	2.306EE-13	9.7885E-14	6.8586E-14
Ra228	6.029EE-21	2.7508E-20	1.0769E-19
Pb206	5.2269E-18	5.5747E-18	3.6378E-18
Pb207	1.0722E-15	1.6859E-15	1.0589E-15
Pb208	4.4347E-10	3.6888E-12	2.0018E-12
Pb210	1.3841E-16	3.0238E-19	1.1829E-19
Th228	7.7910E-10	8.4756E-12	4.9017E-12
Th229	3.5259E-11	2.7278E-12	1.4379E-12
Th230	1.1419E-08	2.6258E-09	2.3998E-09
Th232	6.3415E-11	4.1748E-10	8.7655E-10
Bi209	2.5042E-13	6.6077E-16	2.6878E-16
Ac227	2.8317E-14	3.0968E-14	2.4608E-14
Pa231	8.8076E-10	9.2465E-10	7.0696E-10
U232	1.4693E-07	0.0000	5.9336E-10
U233	4.0461E-08	2.2139E-09	1.0359E-08
U234	0.0010	0.0001	0.0002
U235	0.0003	0.0076	0.0043
U236	0.0005	0.0057	0.0051
U238	0.5864	0.9208	0.8283
Np237	0.0038	0.0006	0.0043
Pu238	0.0096	0.0002	0.0060
Pu239	0.0981	0.0060	0.0410
Pu240	0.0890	0.0029	0.0283
Pu241	0.0155	0.0017	0.0146
Pu242	0.0273	0.0008	0.0098
Pu244	1.779EE-07	2.8648E-08	2.1888E-07
Am241	0.0077	6.4427E-05	0.0021
Am242m	0.0005	8.5336E-07	5.0357E-05
Am243	0.0091	0.0001	0.0020
Cm242	0.0004	2.5898E-05	0.0002
Cm243	0.0000	0.0000	1.2639E-05
Cm244	0.0067	8.5616E-05	0.0010
Cm245	0.0017	5.7217E-06	0.0001
Cm246	0.0009	7.2956E-07	6.1406E-06
Cm247	0.0000	0.0000	1.2059E-07
Cm248	4.0265E-06	7.6916E-10	9.1585E-09
Cm250	1.076EE-12	4.2808E-18	3.7338E-17
Cf249	1.6590E-07	1.6499E-12	4.0567E-11
Cf250	9.5219E-09	2.0419E-12	2.9328E-11
Cf251	3.2032E-10	9.8655E-13	1.4479E-11
Cf 252	8.3754E-12	6.5797E-13	7.5346E-12
H3	3.1829E-07	8.5846E-08	1.0269E-07
Kr81	1.5156E-11	4.2168E-11	7.3446E-11
Kr85	0.0000	3.4448E-05	2.0548E-05
Sr90	0.0009	0.0007	0.0004
Tc99	0.0029	0.0011	0.0011
I129	0.0009	0.0002	0.0003
Cs134	0.0001	0.0002	0.0002
Cs135	0.0051	0.0006	0.0009

Table 7.1: Spent Fuel Compositions

References

[1] Álvarez-Velarde, F., González-Romero, E. M., and Rodríguez, I. M. (2014). Validation of the burn-up code EVOLCODE 2.0 with PWR experimental data and with a Sensitivity/Uncertainty analysis. *Annals of Nuclear Energy*, 73:175–188.

[2] Álvarez-Velarde, F., Martín-Fuertes, F., and González-Romero, E. M. (2008). Analysis of European fuel cycle transition and equilibrium scenarios with LWR and ADS. In *Proc. 10 th Information Exchange Meeting on Actinide and Fission Product P&T*, pages 978–92, Mito, Japan.

[3] Association, W. N. (2017). Nuclear Power in the European Union - World Nuclear Association.

[4] Bae, J. W., Park, G. T., Huff, K., and Chee, G. (2018). arfc/transition-scenarios: Synergistic Spent Nuclear Fuel Dynamics Within the European Union v2.0.0. *Zenodo*.

[5] Baumgaertner, F. (1976). The Purex process for the reprocessing of nuclear fuels with high Pu content and high burn-up. *Kerntechnik*, 18(6):245–252.

[6] Betzler, B. R., Powers, J. J., and Worrall, A. (2017). Molten salt reactor neutronics and fuel cycle modeling and simulation with SCALE. *Annals of Nuclear Energy*, 101(Supplement C):489–503.

[7] Betzler, B. R., Robertson, S., Davidson (nÃľe Sunny), E. E., Powers, J. J., Worrall, A., Dewan, L., and Massie, M. (2018). Fuel cycle and neutronic performance of a spectral shift molten salt reactor design. *Annals of Nuclear Energy*, 119:396–410.

[8] Birkett, J. E., Carrott, M. J., Fox, O. D., Jones, C. J., Maher, C. J., Roube, C. V., Taylor, R. J., and Woodhead, D. A. (2005). Recent developments in the Purex process for nuclear fuel reprocessing: Complexant based stripping for uranium/plutonium separation. *CHIMIA International Journal for Chemistry*, 59(12):898–904.

[9] Boucher, L. (2012). Benchmark Study on Nuclear Fuel Cycle Transition Scenarios Analysis Codes. Technical Report NEA/NSC/WPFC/DOC(2012)16, OECD, Nuclear Energy Agency.

[10] Boucher, L., Velarde, F. A., Gonzalez, E., Dixon, B. W., Edwards, G., Dick, G., and Ono, K. (2010). International comparison for transition scenario codes involving COSI, DESAE, EVOLCODE, FAMILY and VISION. *Actinide and Fission Product Partitioning and Transmutation*, page 61.

[11] Boullis, B. (2015). The French Nuclear Fuel Cycle.

[12] Brown, N. R., Carlsen, B. W., Dixon, B. W., Feng, B., Greenberg, H. R., Hays, R. D., Passerini, S., Todosow, M., and Worrall, A. (2016). Identification of fuel cycle simulator functionalities for analysis of transition to a new fuel cycle. *Annals of Nuclear Energy*, 96:88–95.

[13] CarrÃľ, F. and Delbecq, J.-M. (2009). Overview on the French nuclear fuel cycle strategy and transition scenario studies. In *Proceedings of GLOBAL*, Paris, France.

[14] CNE2 (2015). Reports of the CNE2. Technical report, Commission Nationae D'Evaluation.

[15] Conti, J., Holtberg, P., Diefenderfer, J., LaRose, A., Turnure, J. T., and Westfall, L. (2016). International Energy Outlook 2016 With Projections to 2040. Technical Report DOE/EIA-0484(2016), USDOE Energy Information Administration (EIA), Washington, DC (United States). Office of Energy Analysis.

[16] Dai, Z. (2017). 17 - Thorium molten salt reactor nuclear energy system (TMSR). In Dolan, T. J., editor, *Molten Salt Reactors and Thorium Energy*, pages 531–540. Woodhead Publishing.

[17] Dunn, K., Ahn, T. W., Elmore, R., Huff, K., Oliver, K., and Wilson, P. P. H. (2009). GENIUS v2: An Extensible Platform for Modeling Advanced Global Fuel Cycles.

[18] Dunzik-Gougar, M. L., Juchau, C. A., Pasamehmetoglu, K., Wilson, P. P. H., Oliver, K. M., Turinsky, P. J., Abdel-Khalik, H. S., Hays, R., and Stover, T. E. (2007). Global Evaluation of Nuclear Infrastructure Utilization Scenarios (GENIUS). In *GLOBAL 2007: Advanced Nuclear Fuel Cycles and Systems, September 9, 2007 - September 13, 2007*, GLOBAL 2007: Advanced Nuclear Fuel Cycles and Systems, pages 1604–1611, Boise, ID, United states. American Nuclear Society.

[19] EIA, U. (2018). Annual Energy Outlook 2018. Technical report, US EIA, Washington, DC.

[20] Eschbach, R., Meyer, M., Coquelet-Pascal, C., Tiphine, M., Krivtchik, G., and Cany, C. (2013). New developments and prospects on COSI, the simulation software for fuel cycle analysis. In *Proc. Int. Conf. GLOBAL*.

[21] Fazio, C. (2013). Study on partitioning and transmutation as a possible option for spent fuel management within a nuclear phase out scenario.

[22] Feiveson, H., Mian, Z., Ramana, M. V., and von Hippel, F. (2011). Spent Fuel from Nuclear Power Reactors. An Overview of a New Study by the International Panel on Fissile Materials. *International Atomic Energy Agency*.

[23] Feng, B., Dixon, B., Sunny, E., Cuadra, A., Jacobson, J., Brown, N. R., Powers, J., Worrall, A., Passerini, S., and Gregg, R. (2016). Standardized verification of fuel cycle modeling. *Annals of Nuclear Energy*, 94:300–312.

[24] Freynet, D., Coquelet-Pascal, C., Eschbach, R., Krivtchik, G., and Merle-Lucotte, E. (2016). Multiobjective optimization for nuclear fleet evolution scenarios using COSI. *EPJ Nuclear Sciences & Technologies*, 2:9.

[25] Galeriu, D. and Melintescu, A. (1999). Technical characteristics of the CANDU reactor. Greece.

[26] GauchÃľ, F. (2012). Generation IV reactors and the ASTRID prototype: Lessons from the Fukushima accident. *Comptes Rendus Physique*, 13(4):365–371.

[27] Gidden, M. J. and Wilson, P. P. H. (2016). A methodology for determining the dynamic exchange of resources in nuclear fuel cycle simulation. *Nuclear Engineering and Design*, 310:378–394.

[28] Gregg, R. and Grove, C. (2012). Analysis of the UK Nuclear Fission Roadmap using the ORION fuel cycle modelling code. In *Proc of the IChemE nuclear fuel cycle conference, Manchester, United Kingdom*, Manchester, United Kingdom.

[29] Group, T. H. (1997). Hierarchical data format, version 5.

[30] Guerin, L., Feng, B., Hejzlar, P., Forget, B., Kazimi, M. S., Van Den Durpel, L., Yacout, A., Taiwo, T., Dixon, B. W., Matthern, G., Boucher, L., Delpech, M., Girieud, R., and Meyer, M. (2009). A Benchmark Study of Computer Codes for System Analysis of the Nuclear Fuel Cycle. Technical Report, Massachusetts Institute of Technology. Center for Advanced Nuclear Energy Systems. Nuclear Fuel Cycle Program. Electric Power Research Institute.

[31] Hatch, M. T. (2015). *Politics and Nuclear Power: Energy Policy in Western Europe*. University Press of Kentucky. Google-Books-ID: TrwfBgAAQBAJ.

[32] Heuer, D., Merle-Lucotte, E., Allibert, M., Brovchenko, M., Ghetta, V., and Rubiolo, P. (2014). Towards the thorium fuel cycle with molten salt fast reactors. *Annals of Nuclear Energy*, 64:421–429.

[33] Hinds, D. and Maslak, C. (2006). Next-generation nuclear energy: The ESBWR. *Nuclear News*, 49(1):35–40.

[34] Huff, K. (2017). A Message from the Immediate Past Chair. *American Nuclear Society Fuel Cycle & Waste Management Division*, page 9.

[35] Huff, K. and Dixon, B. (2010). Next Generation Fuel Cycle Simulator Functions and Requirements Document. Technical Report fcrd-sysa-2010-000110, Idaho National Laboratory.

[36] Huff, K. D., Fratoni, M., and Greenberg, H. (2014). Extensions to the Cyclus Ecosystem In Support of Market-Driven Transition Capability. In *Transactions of the American Nuclear Society*, Anaheim, CA, United States. American Nuclear Society.

[37] Huff, K. D., Gidden, M. J., Carlsen, R. W., Flanagan, R. R., McGarry, M. B., Opotowsky, A. C., Schneider, E. A., Scopatz, A. M., and Wilson, P. P. H. (2016). Fundamental concepts in the Cyclus nuclear fuel cycle simulation framework. *Advances in Engineering Software*, 94:46–59. arXiv: 1509.03604.

[38] Hugelmann, D. and Greneche, D. (1999). MELOX fuel fabrication plant: operational feedback and future prospects. In *MOX Fuel Cycle Technologies for Medium and Long Term Deployment (Proc. Symp. Vienna, 1999), C&S Papers Series No*, volume 3, pages 102–108.

[39] IAEA (2008). Guidance for the Application of an Assessment Methodology for Innovative Nuclear Energy Systems INPRO Manual - Overview of the Methodology.

[40] IAEA (2018). Nuclear Power Reactors in the World.

[41] IAEA, P. (2017). *Nuclear Power Reactors in the World*. Number 2 in Reference Data Series. IAEA, Vienna, Austria.

[42] Ignatiev, V., Feynberg, O., Gnidoi, I., Merzlyakov, A., Surenkov, A., Uglov, V., Zagnitko, A., Subbotin, V., Sannikov, I., Toropov, A., Afonichkin, V., Bovet, A., Khokhlov, V., Shishkin, V., Kormilitsyn, M., Lizin, A., and Osipenko, A. (2014). Molten salt actinide recycler and transforming system without and with ThâĂŞU support: Fuel cycle flexibility and key material properties. *Annals of Nuclear Energy*, 64(Supplement C):408–420.

[43] Jacobson, J., Yacout, A., Matthern, G., Piet, S., Shropshire, D., Jeffers, R., and Schweitzer, T. (2010). Verifiable fuel cycle simulation model (VISION): a tool for analyzing nuclear fuel cycle futures. *Nuclear Technology*, 172(2):157–178.

[44] Jorgensen, L. (2017). 19 - ThorCon reactor. In Dolan, T. J., editor, *Molten Salt Reactors and Thorium Energy*, pages 557–564. Woodhead Publishing.

[45] Joskow, P. L. and Parsons, J. E. (2012). The Future of Nuclear Power After Fukushima. Working Paper, MIT CEEPR.

[46] Laidler, J. J., Battles, J. E., Miller, W. E., Ackerman, J. P., and Carls, E. L. (1997). Development of pyroprocessing technology. *Progress in Nuclear Energy*, 31(1-2):131–140.

[47] LeBlanc, D. and Rodenburg, C. (2017). 18 - Integral molten salt reactor. In Dolan, T. J., editor, *Molten Salt Reactors and Thorium Energy*, pages 541–556. Woodhead Publishing.

[48] Leppanen, J., Pusa, M., Viitanen, T., Valtavirta, V., and Kaltiaisenaho, T. (2015). The Serpent Monte Carlo code: Status, development and applications in 2013. *Annals of Nuclear Energy*, 82:142–150.

[49] Martin, G. and Coquelet-Pascal, C. (2017). Symbiotic equilibrium between Sodium Fast Reactors and Pressurized Water Reactors supplied with MOX fuel. *Annals of Nuclear Energy*, 103:356–362.

[50] McCarthy, K. A., Dixon, B., Choi, Y.-J., Boucher, L., Ono, K., Alvarez-Velarde, F., Gonzalez, E. M., and Hyland, B. (2012). Benchmark Study on Nuclear Fuel Cycle Transition Scenarios Analysis Codes. Technical report, Tech. Rep. NEA/NSC/WPFC/DOC.

[51] Merino Rodríguez, I., Álvarez-Velarde, F., and Martín Fuertes, F. (2014). Analysis of advanced European nuclear fuel cycle scenarios including transmutation and economic estimates. *Annals of Nuclear Energy*, 70(null):240–247.

[52] Moore, R. S. and Notz, K. J. (1989). Physical characteristics of GE (General Electric) BWR (boiling-water reactor) fuel assemblies. Technical Report ORNL/TM-10902, Oak Ridge National Lab., TN (USA).

[53] Mourogov, A. and Bokov, P. M. (2006). Potentialities of the fast spectrum molten salt reactor concept: REBUS-3700. *Energy Conversion and Management*, 47(17):2761–2771.

[54] OECD (2009). *Nuclear Fuel Cycle Transition Scenario Studies*. Nuclear Science. OECD Publishing.

[55] Office, U. S. G. A. (2011). Nuclear Material: DOE's Depleted Uranium Tails Could Be a Source of Revenue for the Government. (GAO-11-752T).

[56] Parks, C. V. (1992). Overview of ORIGEN2 and ORIGEN-S: Capabilities and limitations. Technical Report CONF-920430-47, Oak Ridge National Lab., TN (United States).

[57] Passerini, S., Kazimi, M. S., and Shwageraus, E. (2014). A Systematic Approach to Nuclear Fuel Cycle Analysis and Optimization. *Nuclear Science and Engineering*, 178(2):186–201.

[58] Peterson, J., van den Akker, B., Cumberland, R., Miller, P., and Banerjee, K. (2017). UNF-ST&DARDS Unified Database and the Automatic Document Generator. *Nuclear Technology*, 199(3):310–319.

[59] Powers, J. J., Gehin, J. C., Worrall, A., Harrison, T. J., and Sunny, E. E. (2014). An inventory analysis of thermal-spectrum thorium-fueled molten salt reactor concepts. In *PHYSOR 2014*, Kyoto, Japan. JAEA-CONF–2014-003.

[60] Powers, J. J., Harrison, T. J., and Gehin, J. C. (2013). A new approach for modeling and analysis of molten salt reactors using SCALE. Sun Valley, ID, USA. American Nuclear Society, 555 North Kensington Avenue, La Grange Park, IL 60526 (United States).

[61] Riley, A. D., Parkes, P., and Donaldson, N. H. A. (1998). Technology development for future Thorp reprocessing. In *Nuclear recycling. RECOD 98. 5. international nuclear conference on recycling, conditioning and disposal*.

[62] Rykhlevskii, A., Bae, J. W., and Huff, K. (2018). arfc/saltproc: Code for online reprocessing simulation of molten salt reactor with external depletion solver SERPENT. *Zenodo*.

[63] Rykhlevskii, A., Lindsay, A., and Huff, K. D. (2017). Online reprocessing simulation for thorium-fueled molten salt breeder reactor. In *Transactions of the American Nuclear Society*, Washington, DC, United States. American Nuclear Society.

[64] Schneider, E. A., Bathke, C. G., and James, M. R. (2005). NFCSim: A Dynamic Fuel Burnup and Fuel Cycle Simulation Tool. *Nuclear Technology*, 151(1):35–50.

[65] Schneider, M. and Marignac, Y. (2008). *Spent nuclear fuel reprocessing in France*.

[66] Schulz, T. L. (2006). Westinghouse AP1000 advanced passive plant. *Nuclear Engineering and Design*, 236(14):1547–1557.

[67] Serp, J., Allibert, M., Benes, O., Delpech, S., Feynberg, O., Ghetta, V., Heuer, D., Holcomb, D., Ignatiev, V., Kloosterman, J. L., Luzzi, L., Merle-Lucotte, E., UhlÃŋÅŹ, J., Yoshioka, R., and Zhimin, D. (2014). The molten salt reactor (MSR) in generation IV: Overview and perspectives. *Progress in Nuclear Energy*, 77(Supplement C):308–319.

[68] Shay, C., DeCarolis, J., Loughlin, D., Gage, C., Yeh, S., Vijay, S., and Wright, E. L. (2006). EPA US national MARKAL database: database documentation. *US Environmental Protection Agency, Office of Research and Development*.

[69] Smith, J. and Simmons, W. E. (1974). An assessment of a 2500 MWe molten chloride salt fast reactor. *Technical Assessments and Studies Division, Atomic Energy Establishment, Winfrith, Dorchester, Dorset, AEEW*, 956.

[70] Society, A. N. (2017). ANS Nuclear Grand Challenges. Technical report, American Nuclear Society, La Grange Park, Illinois, USA.

[71] Sunny, E. E., Worrall, A., Peterson, J. L., Powers, J. J., Gehin, J. C., and Gregg, R. (2015). Transition Analysis of Promising US Future Fuel Cycles Using ORION. Technical report, Oak Ridge National Laboratory (ORNL), Oak Ridge, TN (United States).

[72] Sutharshan, B., Mutyala, M., Vijuk, R. P., and Mishra, A. (2011). The AP1000tm Reactor: Passive Safety and Modular Design. *Energy Procedia*, 7:293–302.

[73] Torgerson, D. F., Shalaby, B. A., and Pang, S. (2006). CANDU technology for Generation III+ and IV reactors. *Nuclear engineering and design*, 236(14-16):1565–1572.

[74] Tsibulskiy, V., Subbotin, S., Khoroshev, M., and Depisch, F. (2006). DESAE (Dynamic Energy System-Atomic Energy): Integrated Computer Model for Perfoming Global Analysis in INPRO Assessment Studies. In *14th International Conference on Nuclear Engineering*, pages 749–753. American Society of Mechanical Engineers.

[75] Tsoulfanidis, N. (2013). *The Nuclear Fuel Cycle*. American Nuclear Society, La Grange Park, Illinois, USA. 00177.

[76] TÃűpfer, K., Kleiner, M., Beck, U., Fisher, U., van Donhanyi, K., Gluck, A., Hacker, J., Hambrecht, J., Hauff, V., and Hirche, W. (2011). GermanyâĂŹs Energy TurnaroundâĂŞA Collective Effort for the Future. *Ethics Commission for a Safe Energy Supply. On behalf of Federal Chancellor Dr. Angela Merkel*.

[77] Van Den Durpel, L., Wade, D. C., and Yacout, A. (2006). DANESS: a system dynamics code for the holistic assessment of nuclear energy system strategies. *Proceedings of the 2006 System Dynamics Conference*.

[78] Varaine, F., Chenaud, M.-S., Marsault, P., Bernardin, B., Conti, A., Sciora, P., Venard, C., Fontaine, B., Martin, L., and Mignot, G. (2012). Pre-conceptual design study of ASTRID core.

[79] Wigeland, R., Taiwo, T., Ludewig, H., Todosow, M., Halsey, W., Gehin, J., Jubin, R., Buelt, J., Stockinger, S., Jenni, K., and Oakley, B. (2014). Nuclear Fuel Cycle Evaluation and Screening - Final Report. *US Department of Energy*.

[80] Wigeland, R. A., Bauer, T. H., Fanning, T. H., and Morris, E. E. (2006). Separations and Transmutation Criteria to Improve Utilization of a Geologic Repository. *Nuclear Technology*, 154(1):95–106.

[81] Wilson, P. (2009). The Adoption of Advanced Fuel Cycle Technology Under a Single Repository Policy. Technical report, University of Wisconsin – Madison.

[82] Worrall, A. (2013). Utilization of used nuclear fuel in a potential future US fuel cycle scenario. *WM2013, Phoenix, AZ*.

[83] Yacout, A. M., Jacobson, J. J., Matthern, G. E., Piet, S. J., and Moisseytsev, A. (2005). Modeling the Nuclear Fuel Cycle. In *The 23rd International Conference of the System Dynamics Society," Boston*. Citeseer.

[84] Zhao, H., Zhang, H., Mousseau, V. A., and Peterson, P. F. (2009). Improving SFR economics through innovations from thermal design and analysis aspects. *Nuclear Engineering and Design*, 239(6):1042–1055.